# Fabrication of alginate hydrogel scaffolds and cell viability in calcium-crosslinked alginate hydrogel

A Thesis Submitted to the College of

Graduate Studies and Research

in Partial Fulfillment of the Requirements

for the Degree of Master of Science

in the Division of Biomedical Engineering

University of Saskatchewan

Saskatoon

by

Ning Cao

## Permission to use

In presenting this thesis in partial fulfilment of the requirements for a Postgraduate degree from the University of Saskatchewan, I agree that the Libraries of this University may make it freely available for inspection. I further agree that permission for copying of this thesis in any manner, in whole or in part, for scholarly purposes may be granted by the professor or professors who supervised my thesis work or, in their absence, by the Head of the Department or the Dean of the College in which my thesis work was done. It is understood that any copying or publication or use of this thesis or parts thereof for financial gain shall not be allowed without my written permission. It is also understood that due recognition shall be given to me and to the University of Saskatchewan in any scholarly use which may be made of any material in my thesis.

Requests for permission to copy or to make other use of material in this thesis in whole or part should be addressed to:

Head of the Division of Biomedical Engineering

University of Saskatchewan

Saskatoon, Saskatchewan S7N 5A9

Canada

## Abstract

Tissue-engineering (TE) is one of the most innovative approaches for tackling many diseases and body parts that need to be replaced, by developing artificial tissues and organs. For this, tissue scaffolds play an important role in various TE applications. A tissue scaffold is a three-dimensional (3D) structure with interconnected pore networks and used to facilitate cell growth and transport of nutrients and wastes while degrading gradually itself. Many fabrication techniques have been developed recently for incorporating living cells into the scaffold fabrication process and among them; dispensing-based rapid prototyping techniques have been drawn considerable attention due to its fast and efficient material processing. This research is aimed at conducting a preliminary study on the dispensing-based biofabrication of 3D cell-encapsulated alginate hydrogel scaffolds.

Dispensing-based polymer deposition system was used to fabricate 3D porous hydrogel scaffolds. Sodium alginate was chosen and used as a scaffolding biomaterial. The influences of fabrication process parameters were studied. With knowledge and information gained from this study, 3D hydrogel scaffolds were successfully fabricated. Calcium chloride was employed as crosslinker in order to form hydrogels from alginate solution. The mechanical properties of formed hydrogels were characterized and examined by means of compressive tests. The influences of reagent concentrations, gelation time, and gelation type were studied. A post-fabrication treatment was used and characterized in terms of strengthening the hydrogels formed. In addition, the influence of calcium ions used as crosslinker on cell viability and proliferation during and after the dispensing fabrication process was examined and so was the influence of concentration of calcium solutions and exposing time in both media and alginate hydrogel. The study also showed that the density of encapsulated cells could affect the viscosity of alginate solution.

In summary, this thesis presents a preliminary study on the dispensing-based biofabrication of 3D cell-encapsulated alginate hydrogel scaffolds. The results obtained regarding the influence of various factors on the cell viability and scaffold fabrication would form the basis and rational to continue research on fabricating 3D cell-encapsulated scaffolds for specific applications.

## Dedications

I dedicate this work to my parents Jianmin Cao and Suxia Wang for their love, support, and enabling me to become an engineering, my wonderful friends Shifeng Qian, Cam Janzen, Gerry Falk and Donica Janzen for their support and encouragement throughout my master graduate studies.

## Acknowledgements

I thank my supervisors, Dr. Daniel Chen and Dr. David Schreyer, for their patience, support, and excellent guidance through my graduate studies, research, and thesis work. Special thanks to the committee members, Dr. Valerie Verge and Dr. Yen-Han Lin. I thank all the professors that I have taken courses from them and shared their professional knowledge with me. In addition, I thank all my colleagues at the Tissue Engineering Research Group and Cameco MS Neuroscience Research Center for their support and assistance. Also, I thank for the support from the Canadian Foundation for Innovation (CFI) and Saskatchewan Health Research Foundation (SHRF) to the present study.

## Table of Contents

## List of Tables

## List of Figures

Figure Page

# Chapter 1 INTRODUCTION

## 1.1 Tissue Engineering and Hydrogel Scaffolds

### 1.1.1 Tissue Engineering and Strategies

Nowadays, the tissues and/or organs for transplantation mainly come from donations, which, however, cannot meet the clinical needs. Figure 1-1, as an example, shows the organ transplant statistics in the states according to United Network for Organ Sharing (UNOS), i.e., the total number of donated organs, transplants, and the total number of patients on the waiting list from 1995 to 2008. It can be seen that there is a huge gap between the supply and demand for organ and tissue transplantation each year [1-3], which significantly increases year by year. By 2008, there were 100,597 people on the transplant waiting list [4, 5]. In order to meet the tremendous need for tissues and organs transplantation, tissue engineering was greatly motivated to develop and fabricate artificial tissues and organs in the past decade.

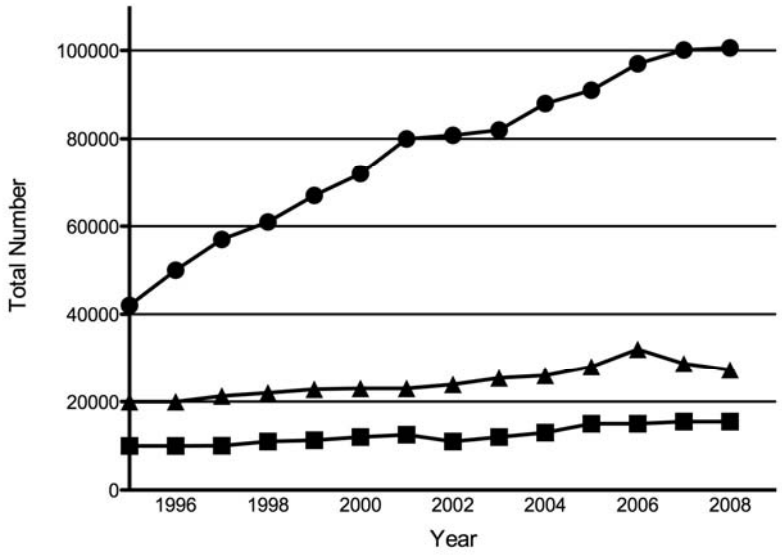


*Figure 1-1 UNOS organ transplant statistics from 1995 to 2008, the total number of donated organs (■), transplants (▲), and the total number on the waiting List (●)*

The basic principles of tissue engineering are illustrated in Figure 1-2, in which the cells from the patient are cultured and expanded, eventually growing into functional grafts or tissues with the help of tissue scaffolds. Tissue scaffolds are three-dimensional (3D) porous, degradable and tissue-like medical implants, which are used to provide synthetic extracellular matrix (ECM), to guide and organize cells into the 3D architecture, and to provide the stimuli directing the growth and formation of functional tissue and/or organs [6]. The principal function of a scaffold is to direct cell behavior such as migration, proliferation, differentiation, maintenance of phenotype, and apoptosis by facilitating sensing and responding to the environment via cell-matrix and cell-cell communications. Typical tissue scaffold should balance its mechanical functions with biofactor delivery. Often this balance presents as a denser scaffold providing stronger mechanical strength and a more porous scaffold providing better biofactor delivery. Porous scaffold also provides more surface areas for cell adhesion and growth. Thus, the architecture of tissue scaffolds is crucial to all tissue engineering applications. Besides, the selection of biomaterials for the scaffold is of importance and dependent on the applications. Bioactive ceramics, for example, were used to develop bone tissue engineering scaffolds because of their favorable biological properties and strong mechanical strength. Due to their inherently-brittle mechanical properties [7, 8], however, they were not commonly used in soft tissue tissue-engineering, such as nerve tissue engineering, where biopolymer-based hydrogel scaffolds would be more suitable.

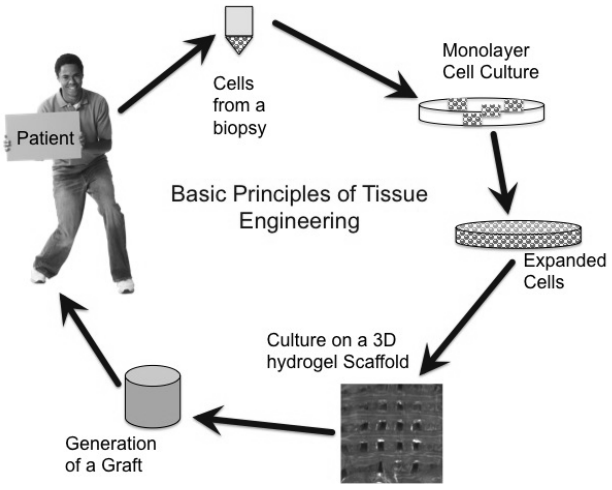


*Figure 1-2 Basic principles of tissue engineering*

### 1.1.2 Biopolymer and Hydrogel Scaffold

Biopolymers have been widely used as common scaffold materials because of their distinct advantages such as controllable biodegradation rate and mechanical properties, good biocompatibility, and ease of processing into desired shapes. Biopolymers are either synthetic or naturally derived. Typical synthetic polymers include poly (lactic acid) (PLA) [9, 10], poly (L-lactic acid) (PLLA) [11, 12], and their copolymers such as poly (DL-lactic-*co*-glycolic acid) (PLGA) [13-15].

Synthetic polymers are attractive for tissue engineering because of their controllability and reproducibility of chemical properties [15], which are important to the dynamics of gel formation, the mechanical and degradation properties of the materials, and the crosslinking density [16, 17]. However, the surfaces of synthetic polymers are hydrophobic, which limits cell adhesion and growth in 3D architecture [18, 19]. Lacking of functional groups on the surface of these polymers limits the possibility of modification. Once implanted in *vivo*, the degradation products of synthetic polymers can easily invoke a chronic immune reaction. In addition, these polymers are typically processed under relatively harsh conditions, which make incorporation and entrapment of viable cells for clinical application difficult, and even impossible [20, 21]. These disadvantages limited their further application in tissue engineering.

Naturally derived polymers include agarose [22, 23], alginate [24, 25], chitosan [26, 27], collagen [28, 29], fibrin [30, 31], gelatin [32], and hyaluronic acid (HA) [33, 34]. Generally speaking, most biopolymers are a class of highly hydrated polymer materials (water content ≥ 30% by weight) [1]. These polymers are composed of hydrophilic polymer chains, and can be crosslinked and gelled by either photopolymerzation or using different crosslinking reagents. The structural integrity of hydrogels depends on the crosslinking bonds formed between polymer chains through various chemical and physical interactions [35, 36]. Most hydrogels used in tissue-engineering applications are biodegradable and can be processed under relatively mild conditions. The hydrogels have many similarities to native tissues or ECM in their mechanical, structural and biological properties, and can be used to form conductive matrix, cellular or biomolecular delivery vehicles [37, 38], or space filling agents [39]. The major concern for hydrogel polymer scaffolds is their low mechanical strength and shape retention failure [36]. Collagen [40, 41], chitosan [42, 43], hyaluronic acid (HA) [44, 45], and alginate [32, 46, 47] are

frequently used naturally derived hydrogel forming polymers in various tissue engineering applications, for they have very similar macromolecular properties to the natural ECM. The aforementioned materials can be found in tissues of adult animals and have shown a favorable interaction with surrounding tissues *in vivo* because of their hydrophilicity and biodegradability. As such, these materials have been widely utilized as hydrogel scaffold materials in tissue engineering. Alginate has been more widely used than other hydrogels in tissue engineering applications especially to form 3D structures that organize cells and present stimuli that can direct the formation of a desired tissue, because of its good biocompatibility with both host and with enclosed cells, and ease of gelation. Currently, the alginate hydrogel has been extensively used in culturing chondrocytes for cartilage repair [48, 49], as well as for hepatocytes [50, 51], and Schwann cells for nerve regeneration [24, 52].

### 1.1.3 Nerve Tissue Engineering

The need for tissue-engineered alternative to nerve graft has been huge, especially in cases like spinal cord injury (SCI) from which many patients suffer due to traffic accidents and trauma each year. This is because that harvested nerve graft is often morbid and of the wrong diameter to the injured nerve. [24, 53, 54] The recovery following nerve grafting has been disappointing, and also because of donor shortage and immunological problems associated with infectious disease that are often encountered in tissue transplantation and nerve grafting. And it is also because that regeneration of adult mammals' axons, which was once thought impossible, is poor and in a disorganized manner after central nervous system (CNS) injury. Researchers have tried various methods to stimulate axonal regeneration and extension into target tissues. For example, there have been experiments on transplantation of peripheral nerves, Schwann cells [55, 56], olfactory ensheathing cells [57, 58], neural stem cells [59], and knock out of gene of encoding Nogo-A/B. These studies have shown that CNS axons can regenerate in a suitable microenvironment, and injured axons can recover part of their function. However, the methods in these studies have limitation for clinical application, such as damage to the donors of peripheral nerves, immunological rejection, difficulty in retaining of exogenous neurotrophic factors at the lesioned site, and potential dangers in genetic manipulation of human tissues.

Biomaterial scaffolds are often used to create substrate within which cells are instructed to form a tissue or an organ in highly controlled way. Various biomaterials, both synthetic and natural

derived, have been employed in nerve tissue engineering for scaffolding. PLLA, chitosan, HA, and alginate have showed potential for incorporation with different therapies to instruct axons to reach to their peripheral targets [60]. Many therapies, such as guided therapies, cellular therapies, and complex therapies that are a combination of methods will be needed have been applied in order to enhance the regeneration and reformation of axons. Cellular based therapies for treating nerve injury often use macrophages to clear debris and glial cells to secrete neurotrophic factors. These methods mainly focus on cell transplantation. Cell transplantations after spinal cord injury are thought to replace lost tissue components, provide re-myelination of denuded axons, provide guidance structures, and express growth factors.

Schwann cell is one of the most thoroughly cell types for transplantation after experimental both peripheral nerve and spinal cord injury. They have been shown to reduce the size of spinal cysts, remyelinate axons and enhance functional recovery in spinal cord injury. Schwann cells produce a number of growth factors that support the growth of axons, including nerve growth factor (NGF), brainderived neurotrophic factor (BDNF), ciliary neurotrophic factor (CNTF), neurotrophin-3 (NT-3), conserved dopamine neurotrophic factor (CDNF) and fibroblast growth factor (FGF) [28, 61]. Additionally, they express axon guidance cell adhesion molecules on their surfaces. Thus, Schwann cells have been employed in many researches including this one to study and stimulate the regeneration of axons.

The Schwann cell and its basal lamina are crucial components in the environment through which regenerating axons grow to reach their peripheral targets. Schwann cells of the injured nerve proliferate; help inflammatory infiltrating cells to eliminate debris, and upregulate the synthesis of trophic and non-tropic factors such as NGF, CNTF, and Laminin. Considering the importance of the Schwann cells in creating an adequate environment for nerve regeneration, researches try to construct of cellular prostheses consisting in a nerve guide seeded with isolated Schwann cells [52, 55].

Schwann cells are the principle neuroglial cells in the peripheral nervous system (PNS). They produce myelin, which has important effects on the speed of transmission of electrical signals and are shown to enhance the regeneration of axons in both the peripheral and central nervous systems. PNS regeneration occurs mainly through a series of reactions produced by activated Schwann cells, providing regenerating axons with numerous neurotrophic factors, cell adhesion

molecules and extracellular matrix components that promote axonal growth. The growth promoting effects of transplanted nerve grafts depend on the presence of viable Schwann cells. In fact, nerve implants devoid of living Schwann cells fail to support central nervous system (CNS) regeneration.

## 1.2 Alginate Hydrogel in Tissue Engineering

### 1.2.1 A Brief Introduction to Alginate Hydrogels

Alginate is a naturally derived polymer and primarily found as a structural component of marine brown seaweed and also as capsular polysaccharides in some soil bacteria. In general, alginate is a linear polysaccharide copolymer composed of (1-4)-linked *β*-D-mannuronic acid (M units) and *α*-L-guluronic acid (G units) monomers. Within the alginate polymer, the M and G units are sequentially assembled in either repeating (-M-M- or -G-G-) or alternating (-M-G-) blocks. The amount and distribution of each unit depends on the sources from which alginate is isolated. Many properties of alginate and its hydrogel such as transmittance, swelling, and viscoelasticity, are significantly influenced by the ratio between M and G units [62]. The carboxylic groups in alginate are capable of forming salt formations such as sodium alginate, where the sodium monovalent ions are attached ionically to the carboxylic groups as shown in .

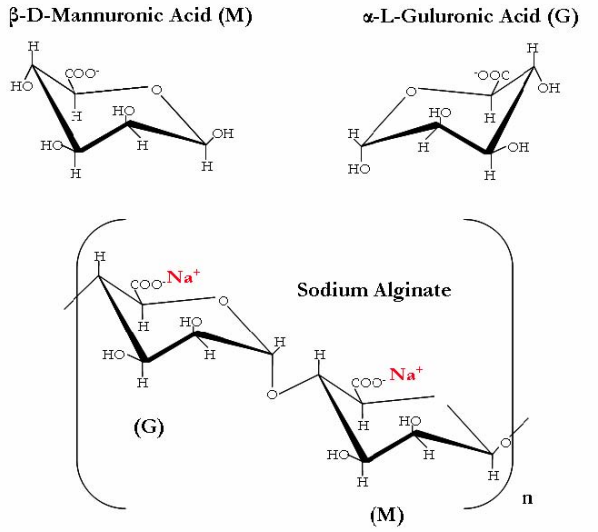


*Figure 1-3 Schematic diagram of β-D-mannuronic acid (M units) and α-L-guluronic acid (G units) monomers, and a -(G-M)- structure sodium alginate*

An important feature of alginate and its derivatives is its gelation in the presence of divalent cations [35] such as calcium ($Ca^{2+}$), through the ionic interaction between these cations and the carboxyl groups located on the polymer backbone. This solution-gel transition process, as illustrated in Figure 1-4, is called crosslinking. The crosslinked hydrogel has an "egg-box" structure. It has been reported that the mechanical strength of these ionically crosslinked alginate hydrogels varied *in vitro* over time. The reason for this phenomenon is that the crosslinking calcium ions in the hydrogel are readily exchanged with the monovalent ions in the surrounding solutions [19]. This process in generally is uncontrollable and unpredictable. The hydrogel has also been formed by covalently crosslinking the alginate chains with polyethylene glycol (PEG) [63] or adipic hydrazide using standard carbodiimide chemistry, in order to precisely control the mechanical and swelling properties of alginate hydrogel [32].

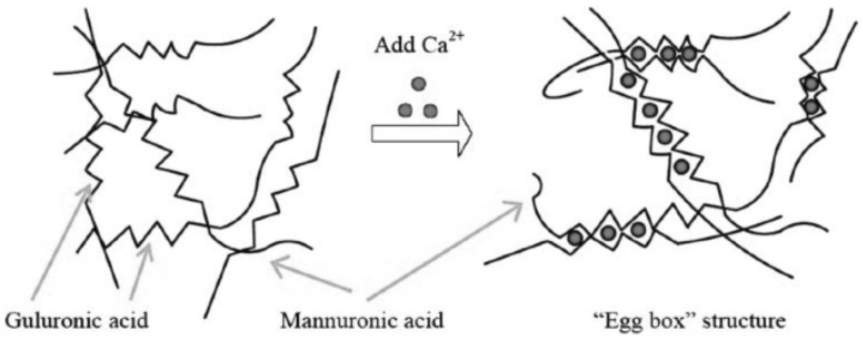


*Figure 1-4 Mechanism of gelation of alginate with presence of calcium ions, forming the "egg-box" structure*

Alginate hydrogels are nontoxic and immunologically inert hydrogel with a high level of biocompatibility and biodegradability. They can easily undergo gelation with divalent cations under the very mild condition suitable for incorporation of biomacromolecules and living cells, thus alginate and its hydrogels have been popularized for pharmaceutical applications like wound dressings [64-66], dental impression materials [67, 68], *in vitro* cell culture and tissue engineering applications. Important applications of alginate hydrogel in tissue engineering include drug delivery applications [32, 69], such as microencapsulation of pancreatic islet cells, creation of a supporting matrix for cells through encapsulation techniques, and alginate-based bioreactors for large-scale manufacture of biological products [46, 47]. Alginate-based microencapsulation is currently a favored approach for cell encapsulation and embedding,

because their properties are tailorable, as has been shown in animal studies and small-scale clinical trials. Besides their good biocompatibility with both host and with enclosed cells, their quality can be constantly ensured by sterile filtering sterilization, or by heat sterilization under special conditions [70]. Alginate hydrogels also have a wide application as rate-controlling excipients in drug delivery systems, as a matrix for biomolecules, and as an excipient in pharmaceutical preparations for local administration [32, 71, 72]. Alginate can be prepared in either neutral or charged form, and so it is compatible with a broad variety of substances. Depending on the pH of the media, alginate has the ability to form two types of gel, an acid or an ionotropic gel, which provides a large variation of physicochemical properties and the swelling process to activate the release of drugs [73]. The concentration of alginate and the proportion of the G units can also influence the drug release rate besides the types of the gel form and its physical thickness. Alginate-cell suspensions may also be gelled *in situ*, to accomplish cell transplantation with minimally invasive surgical procedures [74].

However, due to some drawbacks in its properties, alginate has also shown its limitations in tissue engineering applications. For example, the alginate hydrogels typically have uncontrollable degradation kinetics due to the loss of divalent ions and subsequent dissolution of the gel by releasing high and low molecular weight alginate struts [75]. Although reports showed the degradability of low molecular weight (<80KDa) alginate, the molecular weights of many alginates used in tissue engineering are typically above the renal clearance threshold of the kidney [76]. There are a few attractive approaches to control the degradation manner of alginate hydrogels, such as the isolation of polyguluronate blocks with molecular mass of 60KDa from alginate chain, partially oxidation [77], and covalent crosslinking with adipic dihydrazide. By controlling the crosslinking density, the gelation, mechanical and degradation properties of these polymers could be well controlled. Also, use of a high calcium concentration to crosslink alginate is reported to inhibit the growth of cells in culture. Other drawbacks of alginate hydrogels are the lack of specific interaction between mammalian cells and protein adsorption due to its hydrophilic character [7]. For improvement, alginate hydrogel was modified with lectin or RGD peptides on carboxylic acid to enhance cell adhesion [78]. These modified alginate gels have been proven useful for the adhesion, proliferation, and differentiation of cells in culture. Alginate has also been mixed with other materials to enhance its biological performance as well

as mechanical strength. For example, an alginate/chitosan based scaffold has been investigated in many tissue engineering areas, such as bone repair [18, 79, 80], and drug release [81, 82].

### 1.2.2 The Methodology of Hydrogel Formation

A number of methods have been developed and reported in the literature to form the alginate hydrogels in tissue engineering applications. Most of these methods are based on the strategies of internal gelling and diffusion gelling. In the first strategy, i.e., internal gelling, the calcium chloride solution is introduced into the reservoir of alginate and the gelation starts at the interface of two reagents, then gelation proceeds into the alginate solution as calcium ions diffuse into the alginate body. The drawbacks for this strategy are the longer gelation time than the first one as well as the difficulties in the control over scaffold structure. In the second strategy, an alginate solution is typically added to a reservoir of divalent ions such as a calcium chloride solution and then the gelation process starts from the outermost layer of alginate as the calcium ions diffuse into the core of the material. This method is mostly used for fabrication process such as polymer deposition because of the advantages of relatively spontaneously gelation, and uniform gel internal structure. With the use of alginate in a variety of fabrication techniques, this method shows the potential to fabricate tissue scaffolds with complex architecture. However, the main drawback of this method is the influence of buoyancy, which has a negative effect on the accuracy of the polymer deposition during fabrication. Besides, the presence of high concentration calcium ions is a challenge for the incorporation of living cells and biomolecules in the biofabrication process, which is also the issue being addressed by the present study. This thesis focused on how this strategy would cooperate with dispensing fabrication and how this would influence cell viability during and after the fabrication.

Besides these two strategies, there are some other methods used to form hydrogel scaffolds. One method is to mix the calcium ions and alginate by using mechanical forces. For example, it has been reported that aqueous alginate was mixed with calcium gluconate solution using homogenization to distribute the calcium ions throughout the solutions in order to form an injectable alginate hydrogel [83, 84]. The other method is to pump the alginate and calcium chloride solutions back and forth in two syringes connected by a three-way stopcock until the elastic hydrogel is obtained [85]. The advantage of this method is that uniform gelation can be obtained. However, due to the mechanical force, mainly shear stress, that the solution-gel

mixture was exposed to, its internal structure could be broken and damaged, which weakens the mechanical strength of the formed hydrogel.

### 1.2.3 Mechanical Properties of Alginate Hydrogel

As employed scaffolding material, the mechanical properties of alginate hydrogel determine the capability of scaffold formation and its porous structure and specific applications in tissue engineering. Also, it has been reported that the mechanical properties of alginate influence cell proliferation, differentiation, location, and morphology [86, 87]. Thus, to study the mechanical properties of alginate hydrogel is important for scaffold fabrication in tissue engineering. Common crosslink reagents include calcium chloride, barium chloride, calcium sulfate, and tyrosinamide; and their gelation rates vary. For example, calcium sulfate crosslinking kinetics are difficult to control, thus leading to nonuniform gel structures; while calcium chloride provides alginate with a relatively fast gelation rate, resulting in a crosslink density [23] and a polymer concentration gradient within gel beads. Researchers have studied the mechanical behavior of alginate with different crosslinkers under various conditions. It has been reported for alginate hydrogels ionically crosslinked with $Ca^{2+}$ and covalently crosslinked with adipic dihydrazide (AAD) [88, 89], methyl ester, L-lysine (Lys), or poly-(ethylene glycol) (PEG) [90, 91] diamines that the mechanical properties depends on the interchain crosslinks and the molecular weight of the crosslinkers. The covalently crosslinked hydrogels all showed inflection points in compression tests, and the value of the inflection point decreased with the increasing molecular weight of crosslinking molecules [92]. Also, the shear moduli of $Ca^{2+}$ crosslinked hydrogels were normally lower than those of covalently crosslinked hydrogels.

As mentioned above, the crosslinking happens on the $\alpha$-L-guluronic residues (G residues), so the mechanical properties highly depend on the ratio of G residues in its sequence and the molecular weight of alginate. Generally speaking, alginate with high M content produces weak, elastic gels with good freeze-thaw behavior, and high G content alginate produces strong brittle gels with good heat stability. While high MGMG content alginate, whose M/G ratio is approximate to one, zips with $Ca^{2+}$ ions to reduce shear [93]. Thus, it used to be believed that alginates with a high content of guluronic acid (G) blocks provide higher strength compared to those rich in mannuronate (M) because of the stronger affinity that G residues showed. However, it has been reported in some studies that high M content alginate can produce stronger hydrogel at either low

or very high $Ca^{2+}$ concentrations ( $[Ca^{2+}]$ ). These results suggested that as long as the average length of polysaccharides are not too short, the properties of the formed hydrogel are correlated with the average length of G chains and not necessarily with the M/G ratio because of the -(M-G)- structure along the chains [94].

The tensile and compression properties of alginate hydrogels also highly depend on the sources of the alginate polymer, as well as the gelation rate in the crosslinking process. Notably, the gelation rate of alginate also depends on the temperature and pH of the solution. Normally, a higher gelation rate will result in shorter gelation time, and the alginate gel that is formed will be less strong. The mechanical properties also increase with increasing concentration of either crosslinking reagent[95]. Due to the loss of $Ca^{2+}$ in the aqueous environment, the mechanical properties of alginate hydrogel are also time dependent. It is reported in some cases that the elastic modulus of alginate hydrogel decreases significantly once incubated or immersed in a physiological environment, for example, losing 60% of mechanical strength within the first 15 hours [96]. In most cases where cells were encapsulated in the gel, the elastic modulus decreased slowly in the first few weeks of incubation due to the loss of calcium ions, and then started to increase. The reason for phenomenon is due to the fact that cell matrix increases within the gel in the first few weeks of incubation [97]. These studies showed that the mechanical properties depend on the source of alginate, G/M ratio, gelation rate, and crosslink density.

The mechanical properties of the microenvironment can influence the behavior of a large variety of cells. It used to be believed that the mechanical properties of alginate hydrogel were not directly responsible for regulating encapsulated cell proliferation, but that the calcium ions released from the crosslinked gels or the presence of alginate are responsible instead. However, recent research reported that there were no observed differences in cell growth for non-encapsulated cells cultured with and without alginate hydrogels, which indicated that the presence of calcium-alginate and calcium released from the gel were not responsible for the lack of proliferation that has been seen [87]. Studies of neural stem cells (NSCs) cultured in alginate hydrogels also confirmed that the mechanical properties of 3D scaffold significantly impacted both the proliferation and neuronal differentiation of encapsulated NSCs, where the elastic modulus of the hydrogel is controlled by varying the concentrations of alginate and calcium. It

has also been observed that the influence of the mechanical properties are also depend on the encapsulated cell type and cell density [86, 87].

In most studies the hydrogel scaffolds were used for either space filling or injection, where the structure of the scaffold was not required. Those hydrogels were mechanically soft and weak, and their mechanical properties were measured and characterized by shear modulus. In order to fabricate a 3D porous hydrogel scaffold, the hydrogel scaffold needs to be strong enough to hold its shape and structure. The difference in mechanical properties would affect the proliferation and other biological activities of encapsulated cells. For this reason, the mechanical properties of alginate hydrogels were studied and measured using a compressive test in this thesis.

### 1.3 Biofabrication of Tissue Scaffolds

Tissue engineering is, by combining cells, scaffolds and bioactive agents, designed to develop methods to restore, maintain, or improve tissue function of those damaged tissues. 3D scaffolds are the most fundamental vehicles in tissue engineering to deliver the cells and bioactive agents and to guide tissue formation both *in vitro* and *in vivo*. To this end, scaffolds should have characteristics such as good biocompatibility, controllable biodegradability, interconnected pores with proper pore size, adequate mechanical properties, etc [98].

Many techniques have been developed to fabricate 3D porous architectures to fill this role. The main techniques for scaffold fabrication include solvent casting [99, 100], particulate leaching techniques [101, 102], gas foaming [103-105], phase separation [106, 107], electrospinning [108, 109], rapid prototyping (RP) techniques [110, 111], melt molding [112, 113], porogen leaching, fiber mesh, fiber bonding, self assembly, membrane lamination, freeze drying [114, 115], etc. The freeze drying technique for example is based upon the principle of sublimation to fabricate porous scaffolds. The typical process would be to dissolve the polymer into a solvent in order to form a solution of desired concentration. Then the solution is frozen and solvent will be removed by lyophilization under a high vacuum. In this method, the pore size and porous structure can be controlled by the freezing rate, pH, and temperature. However, the small pore size formed in this technique is a concern for some applications, and also, this technique is a time consuming technique because of the utilization of lyophilization [116, 117].

Rapid prototyping (RP), also known as solid free form (SFF), can rapidly produce 3D object by using a layer-manufacturing method. RP techniques have no restrictions on microstructure control and consistency in contrast with other fabrication techniques. The RP technique is a computerized fabrication approach that can rapidly produce a highly complex 3D tissue engineering scaffold by laying down multiple, precisely fabricated two dimensional layers. For example, the image of a bone defect can be obtained and then developed into a 3D computer-assisted design (CAD) model, which is then mathematically transformed to a series of layers. Typical rapid prototyping techniques include selective laser sintering (SLS), three dimension printing (3DP), and fused deposition modeling (FDM) [118, 119]. The RP technique has advantages over other fabrication techniques, as shown in . The key one is its precise control over the scaffold architecture, such as size, shape, inter-connectivity, porosity, and geometry, thus providing a means to fabricate the scaffold with controlled mechanical and biological properties.

*Table 1-1 Comparison of different techniques for the tissue engineering scaffolds fabrication*

| Methods | Advantages | Drawbacks |
|---|---|---|
| Solvent Casting/Particulate Leaching | Controlled porosity, pore size, inexpensive | Limited mechanical properties, residual solvents or porogen materials |
| Phase Separation | Ease to combine with other techniques, ability to keep the activity of biomolecules | Difficulty to precisely control scaffold morphology |
| Freeze Drying | Simplicity of utilization, no high temperature or leaching | Small pore size, and long processing time |
| Eletrospinning | Controllable porosity, pore size, and fiber diameter | Limited mechanical properties, decreased pore size with increasing thickness |
| Rapid Prototyping | Excellent controlled geometry, porosity, good repeatability | Expensive equipment, limited polymer type |

Dispensing based rapid prototyping techniques have been already widely used in tissue engineering to deliver the scaffold fabrication material because of its precisely control over microstructure, good repeatability, capacity for adapting to different materials states, from liquid to thick paste, and relatively mild fabrication condition such as low operating temperature, no toxic solvent needed, and fast and efficient material processing. Dispensing based RP approaches used in tissue engineering include precision extrusion manufacturing, 3D plotting, 3D printing, cell assembling, direct writing, photo-patterning, robotic dispensing, and micro-syringe deposition, etc.

### 1.3.1 Dispensing Based Polymer Deposition

The dispensing based polymer deposition technique is promising not only for mimicking the anatomical geometries but also for the possibility of placing cells, growth factors, and/or peptides as desired within a 3D structure [120]. In order to place cells into the scaffolds, several RP techniques such as jet-based printing, dispensing-based polymer deposition, and laser forward transfer techniques have been developed in the literature. Dispensing-based polymer deposition has shown more promising than other techniques because of its fast and efficient material processing. In a dispensing system, a pneumatic or other volumetrically driven dispenser is used to deposit the scaffold material solution with/without the cells in a controllable manner [85, 121, 122]. One advantage of this fabrication technique rests on its controllability over the structure, porosity, and connectivity of 3D scaffolds.

A variety of dispensing-based polymer deposition systems have been developed, including a low temperature double-nozzle dispensing assembling system [123], multiple-nozzle dispensing system [120], and a hydrodynamic spinning approach for synthesizing hydrogel fibers of different diameters in a multiphase coaxial flow [124]. A typical computerized dispensing based polymer deposition system contains a computer, a dispenser controller, a position controller guiding the nozzle movement in X-Y-Z directions, and temperature controller, as shown in Figure 1-5.

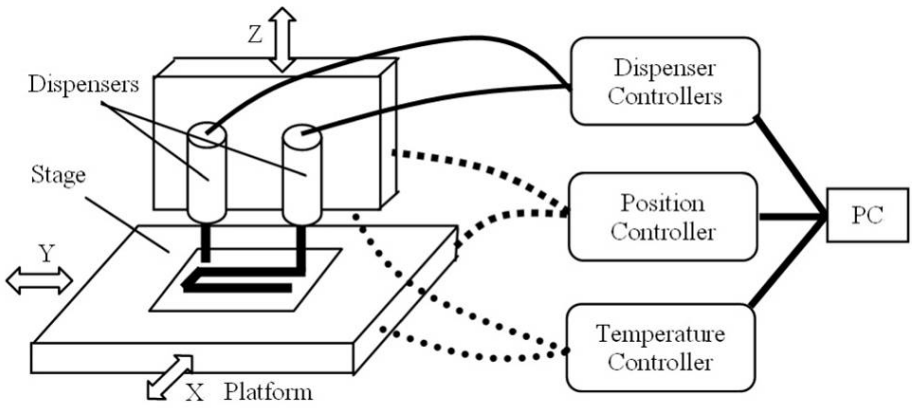


*Figure 1-5 Schematic of a dispensing-based polymer deposition system*

There are three kinds of dispensing strategies according to the dispenser type, which are employed in dispensing based RP approaches. These are time pressure, rotary screw, and positive displacement [125], shown in Figure 1-6. The time-pressure dispensing strategy utilizes pressurized air to drive fluid out of the needle. The amount of fluid dispensed depends on the magnitude and duration of pressurized air, the type and size of the needle, and the viscosity of the material. This strategy is the most popular dispensing approach among these three for tissue engineering because of its flexibility and capacity for adapting materials of different states including liquid [126], pastes [127], and semi-molten polymers [128], easy maintenance, and simple operation. However, the timed-pressure strategy has drawbacks including the significant influence of fluid viscosity, and air compressibility in the syringe on the amount of the fluid dispensed [129].

The rotary-screw dispensing strategy utilizes the rotation of a motor-driven screw to move fluid down a syringe and then out of a needle. The merits of this strategy include precise manipulation of small fluid volume and the improved control in the fluid amount dispensed through the use of a rotary screw. Given the fact that a large pressure can be built in the fluid at the syringe bottom, depending on the flow behavior of the fluid being dispensed, the fluid amount dispensed is also affected by the fluid flow behavior. In positive-displacement dispensing, the fluid in the syringe could be precisely manipulated by the linear movement of a piston. However, this advantage can be lost for dispensing small amounts of fluid due to the fluid compressibility.

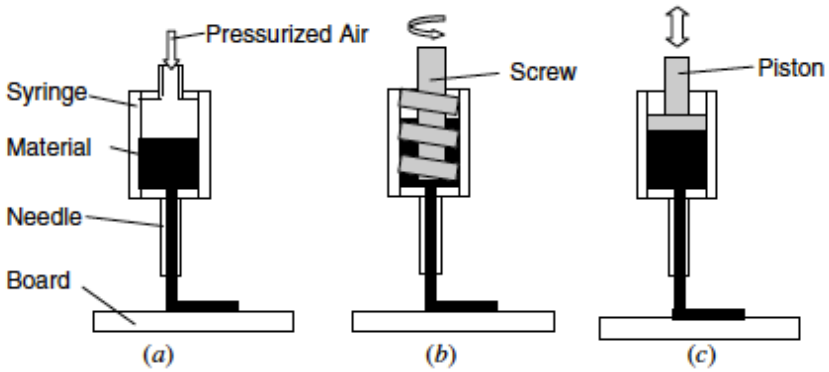


*Figure 1-6 Schematic of fluid dispensing approaches, (a) time pressure, (b) rotary screw, and (c) positive displacement*

### 1.3.2 Factors Influence the Fabrication

One advantage for the RP technique over other techniques is its ability to precisely control the internal structure of the scaffold and its consistency. However, designing the control process to persistently fabricate such a scaffold is a challenging task. It has been reported that in the dispensing-based fabrication process, the flow rate of biopolymer dispensed and the pore size and porosity of the scaffold can be affected by several factors such as temperature, the air pressure applied to the process, and the flow behavior of the biopolymer. Models for both Newtonian fluid and non-Newtonian fluid were developed in order to achieve precise control of the fabrication process. In most models, the diameter of the fabricated struts depends on the volumetric flow rate through the needle, which is a function of the diameter of nozzle, the applied air pressure, the length of the needle, the height of the needle, the fluid behavior, and even the shape of the needle used. So these are also the factors that influence the printing resolution.

In the research that has been reported, for example, sodium alginate was deposited by the pneumatic micro-valve, which is capable of depositing sodium alginate concentration up to 3% (w/v) [130]. In this study, a range of nozzle diameters of 250 μm, 330 μm, and 410 μm and pressures from 8 psi to 32 psi were used in order to fabricate 3D tissue scaffolds. The deposition flow rate is directly proportional to the operating pressure and the nozzle diameter; however, it is inversely indirectly proportional to the sodium alginate concentration according to the

experiment. Thus, the controllability of depositing alginate is crucial to controlling the size and structure of the scaffold, strut diameter, and the porosity of the scaffold.

Besides these factors, the speed of needle movement has been reported to be a crucial influence on the diameters of the formed struts, and on the structure of the scaffolds. As shown in Figure 1-7, if the speed is slower than the appropriate speed range for the fabrication, it was hard to form a straight line because of the action of fluid compression in the strut. On the other hand, if the speed is too fast, the strut can be broken because of the tension [131].

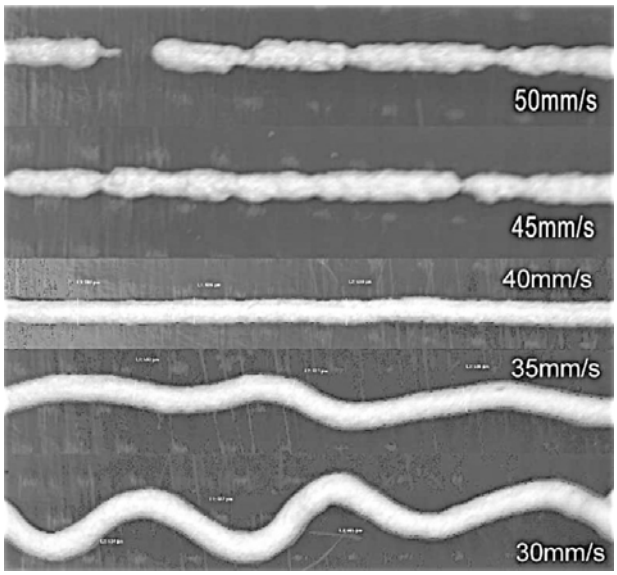


*Figure 1-7 Struts formed by using different speeds [131]*

It has also been reported that the diameter of the struts would differ from the diameter of the nozzle used in fabrication, depending on the speed of the needle movement. Specifically, if the speed is too fast, the diameter of the strut would be smaller than the one of the nozzle; and in contrast, if the speed is too slow the strut diameter would become bigger than the one of the nozzle [130].

### 1.3.3 Influence of Nano-Particles on the Flow Behavior

Biofabrication is a process to fabricate the complex tissue engineered products such as tissue scaffolds by using biomaterials combined with the living cells and/or biomolecules. Typical applications of these cells and biomolecules include drug delivery [132], modifying the chemical

and biological properties of the biomaterials used to fabricate the scaffolds [133, 134], and providing the growth factors and stimuli to promote the regeneration and proliferation of the target tissues and organs [135]. Nano-particles composed of hydroxyapatite have also been mixed with scaffolding materials in order to enhance the mechanical properties of the scaffold [136] or to enhance contrast in resonance imaging [137]. By controlling the placement of these particles within the scaffold structure, it is possible to create a gradient of growth factors to direct the growth of cells and formation of the desired tissues and organs. Cells can be also labeled by loading the nano-particles inside of them or by attaching them to the cell membranes. These labeled cells could be manipulated to be printed into specifically designed two dimensional or 3D patterns *in vitro* [138, 139] and then imaged as the tissue develops.

As mentioned before, the flow behavior, typically characterized by viscosity, can influence the fabrication process and the structural parameters of the scaffold indirectly. It has been reported that the viscosity of biopolymers such as collagen, alginate, and chitosan is a function of shear rate and that viscosity increases with the polymer concentration and the pressure applied on the solutions [130]. The presence of living cells, biomolecules, and nano particles could change the concentration of the solution, which would affect the viscosity of the solution.

### 1.3.4 Cell Viability in the Biofabrication Process

Incorporation of cells during the biofabrication process has recently been drawing considerable attention from researchers. Various biofabrication methods have been explored and developed, including dispensing based cell deposition, solvent casting, and freeze-drying. Due to the harsh conditions involved in each of the techniques, cell damage occurs during and even after the fabrication process in most cases. Once cells are damaged, they will either recover through their own recovery mechanism or stay dysfunctional till they die eventually. In order to achieve the goal of incorporation of living cells, the mechanism and impacts of the cell damage that happens during and after the fabrication process need to be explored.

Dispensing based cell deposition, in which a pneumatic or other volumetrically driven dispenser is used to deposit the material, has been considered as a promising technique because of its fast and efficient material processing and manipulating capacity. In this process, cells are encapsulated in a biocompatible material and then extruded and delivered to designated targets in a controlled manner. In a pneumatic dispensing based deposition setup, the cells suspension

flows through a needle under pressurized air. During this process, cells are exposed to mechanical forces such as pressure and shear stress. Once these forces exceed certain thresholds and/or the forces are applied beyond certain time periods, cells will be harmed or damaged irreversibly, resulting in the loss of cell functions. Studies have shown that both air pressure and needle diameter significantly influenced cell damage in the dispensing based polymer deposition process. Generally speaking, for a direct cell writing system, both decreasing nozzle diameter and increasing applied dispensing air pressure lead to the increase of mechanical stresses, thus decreasing cell viability [121, 140]. The results of some studies showed that the percent of cells damaged during the fabrication process increases with the length of the needle, which determines the time period cells are exposed to the applied air pressure. It is also observed that the cell damage during the fabrication process is unevenly distributed along the direction of the needle radial. Cells located near the needle wall are more vulnerable than those near the center because the shear stress and exposure time cells experienced in the needle vary in the radial direction. All the conclusions suggest that the process parameters can be optimized to minimize the cell damage during the fabrication process [141].

### 1.4 Research Objectives

This research is aimed at conducting a preliminary study on the dispensing-based biofabrication of 3D cell-encapsulating alginate hydrogel scaffolds, which are potentially to be used in nerve tissue engineering. The objectives of this research are in particular (1) to study the properties of materials used for this fabrication process, (2) to study the factors that influence the scaffold fabrication process, and (3) to investigate the effects of calcium ions on cell survival and functions occurring during and after the fabrication process.

Objective 1: Study on Alginate Hydrogel Mechanical Properties

The mechanical properties of the alginate hydrogel has been shown to influence both the structure of the fabricated scaffold and the proliferation and metabolism of encapsulated cells. The influence depends on the source of the alginate, the crosslinking density, the method of crosslinking, and the type of encapsulated cells. Although the influence of alginate on encapsulated neural stem cells and bone marrow cells has been reported, the effects on the Schwann cells used in this project haven’t been explored. Also, in most reported studies, the mechanical properties were measured and characterized by rheological measurements,

particularly for injectable scaffolds. These studies are limited to the low crosslink density and weak, soft mechanical properties of the alginate hydrogel. As a result, the alginate hydrogel was fragile and cannot be fabricated into porous structures with integrity under the effect of gravity. Besides, the mechanical properties of alginate hydrogel were usually characterized by means of the shear modulus through rheological measurements in the previous studies, the compressive properties of the hydrogel, which are important to various tissue engineering applications, have not been documented in the literature.

Thus, the mechanical properties of alginate hydrogel with maximum crosslink density were characterized by compression elastic modulus in this study. Also, the effects of the key factors influencing the mechanical properties of alginate hydrogel was studied, including concentration of both alginate and calcium, the proportion of these two reagents, the gelation time and gelation methods. The mechanical properties of alginate hydrogel bulk at various concentrations were tested and measured to investigate the elastic modulus and yield strength.

Objective 2: Study on the Scaffold Fabrication Process

This objective is to advance the knowledge required to fabricate 3D hydrogel scaffolds. In this study, a dispensing-based printing system was used to fabricate the designed 3D scaffolds. Alginate solution was used as the biopolymer for the fabrication process, which is capable of being printed at ambient temperatures in aqueous solution. Calcium chloride was selected as the crosslinking reagent to gel the alginate.

There are various factors can influence the scaffold fabrication process and thus the scaffold fabricated. The effects of parameters such as nozzle diameter, applied air pressure, solution viscosity, and types of nozzle on scaffold fabrication were studied and investigated. This thesis focused on the effects of air pressure and the moving speed of the nozzle on the printing resolution. Then, a porous 3D hydrogel scaffold was fabricated based on the knowledge obtained from this study.

Objective 3: Study of the Effects of Calcium Ions on Cell Viability

There can be many sources such as process-induced force and calcium ions causing cell damage in the scaffold fabrication process, in which cells are incorporated. Since the cell damage caused by calcium ions was never systemically studied before, the concentrations of calcium chloride

solution and cell density used in the previous studies were chosen based on the researchers' experience. The effect of alginate and calcium chloride concentrations on the viability and proliferation of encapsulated cells is a void in the literature. Also, the influence of cell density on viability and proliferation during and after the fabrication process needs to be studied. In the present study, Schwann cell lines were employed for its wide applications in the nerve tissue engineering.

### 1.5 Thesis Outline

The second chapter of this thesis presents the studies and discusses the mechanical properties of alginate hydrogel bulk. In this chapter, the effects of concentration of alginate and calcium, the gelation time, and gelation method are investigated. The third chapter introduces the fabrication process of a 3D alginate hydrogel scaffold. Also, the crucial factors such as fluid viscosity, applied air pressure, nozzle type, and nozzle diameter are investigated for controlling the strut diameters, scaffold pore size, and porosity. In the fourth chapter, the effects of calcium ions in the aqueous solution and alginate hydrogel on the encapsulated cells during and after the fabrication is investigated and studied. The influence on the proliferation of encapsulated cells is discussed. The influence of encapsulated cells on the viscosity of alginate solution is also presented in this chapter. The last chapter summarizes the research work of this thesis and presents the conclusions with recommended future work.

# Chapter 2 MECHANICAL PROPERTIES OF ALGINATE HYDROGEL

## 2.1 Sodium Alginate

Sodium alginate, as the most common alginate salt derivative, is soluble in water and once dissolved, forms viscous solutions. The properties of the solution depend on the concentration and molecular weight of the biopolymer. Sodium alginate, as a form of flavorless gum, is often used in the food industry to increase viscosity. Sodium alginate can be crosslinked in aqueous solution with the presence of calcium ions. The solution-gel transition is caused by calcium ions exchanging with sodium ions, and binding the guluronic residues together to form crosslinks in the material. These crosslinks have an "egg-box" structure [142], as previously shown in Figure 1-4, and show viscoelastic solid behavior. Because of its biocompatibility and low toxicity, and spontaneous gelation, alginate gel crosslinked with calcium ions ($Ca^{2+}$) has been widely applied for variety of tissue engineering studies. Previous studies show that the mechanical properties of alginate hydrogel have an influence on both the structure of the fabricated scaffold and the proliferation and metabolism of encapsulated cells [86]. Unfortunately, these studies were all focusing on shear modulus, which is a quantity for describing the stiffness of the material and its response to a shear strain, and little was reported regarding the compressive properties of alginate hydrogel, which is of importance in order to form 3D structure in the fabrication of hydrogel scaffolds, as concerned in the present study. This chapter presents a study on compressive properties of alginate hydrogel, with emphasis on identifying the influence of the fabrication process parameters.

## 2.2 Materials and Methods

Low viscosity sodium alginate (Sigma, St. Louis, MO), molecular weight range 12,000~80,000 mannuronic acid 61% and guluronic acid 39%, aqueous solutions with concentration of 2% and 4% (w/v) were prepared using deionized water. Calcium chloride (Sigma, St. Louis, MO), dissolved in deionized water, were used as the crosslinker to gel sodium alginate aqueous solution. Dulbecco's Modified Eagle Medium (DMEM) solution (Invitrogen, Carlsbad, USA)

were used as the physiological environment to study the swelling and degradation properties of alginate specimens (as prepared below) *in vitro*.

### 2.2.1 Preparation of the Specimen

The specimens used in this study were prepared in two different methods. In both methods, the solutions of the two reagents, alginate and calcium chloride, were filled into a custom-made cylindrical Teflon mold (10 mm diameter × 20 mm length) at a volume ratio of 2:1 (alginate: calcium chloride), to crosslink at room temperature. In the first method, the hydrogels (n = 4) were removed from the mold after 6 hours and the specimens were then placed into a calcium chloride solution for further crosslinking, which is referred as to the post-fabrication treatment. Specifically, a solution with concentration of calcium ions ( $[Ca^{2+}]$ ) 100 mM at 25°C was used and specimens were treated for 24 hours. According to the concentration of each reagent used in this study, the specimens were divided into four groups, i.e.,

Group 1-1 was the hydrogel specimens made from 2% alginate and 100 mM $[Ca^{2+}]$ solution,

Group 1-2 was the hydrogel specimens made from 2% alginate and 200 mM $[Ca^{2+}]$ solution,

Group 1-3 was the hydrogel specimens made from 4% alginate and 100 mM $[Ca^{2+}]$ solution,

Group 1-4 was the hydrogel specimens made from 4% alginate and 200 mM $[Ca^{2+}]$ solution.

In the second method, the specimens were made by mixing both reagents solution in the custom designed Teflon mold at the volume ratio of 2:1 (alginate: calcium chloride) crosslinking for 24 hours, and then rinsed in deionized water for three times. No post-fabrication treatment was applied to these specimens; and these specimens were used as a control group as compared to those with the post-fabrication treatment. According to the concentration of each reagent used in this project, the specimens can also be divided into four groups,

Group 2-1 was the hydrogel specimens made from 2% alginate and 100 mM $[Ca^{2+}]$ solution,

Group 2-2 was the hydrogel specimens made from 2% alginate and 200 mM [$Ca^{2+}$] solution,

Group 2-3 was the hydrogel specimens made from 4% alginate and 100 mM [$Ca^{2+}$] solution,

Group 2-4 was the hydrogel specimens made from 4% alginate and 200 mM [$Ca^{2+}$] solution.

The hydrogels formed by means of both methods were cut into cylindrical shape of 10 mm diameter × 10 mm length for subsequent mechanical tests.

### 2.2.2 Apparatus for Measuring Mechanical Properties

The mechanical tests were all performed on a desktop measurement system, ElectroForce® 3100 test instrument (Bose Corporation, ElectroForce® Systems Group, USA), which provides ± 22 N (5 lb) linear force with a frequency response of 100 Hz, and a displacement stroke of 5 mm (0.2 in). The transducer of this instrument also has the capacity of providing high resolution of a minimum 6 mN (0.001 Lb) controllable peak-to-peak force and minimum 0.0015 mm (0.00006 in) controllable peak-to-peak displacement. Because of the aforementioned features, this instrument is particularly suitable for tissue mechanics research, micro indentation of cartilage and other soft tissues, dynamic mechanical analysis (DMA) of tissues, elastomers and other soft materials [143].

The measurement system is controlled by the WinTest® digital control system on a customized computer through two digital controllers. The hardware of this instrument includes a load sensor with a maximal force range ± 22 N (5 lb), a mover with a displacement range ± 2.5 mm (0.1 in), a chamber that provides a sterilized and isolated environment as a bioreactor, and a frame to hold all these parts together, as shown in Figure 2-1.

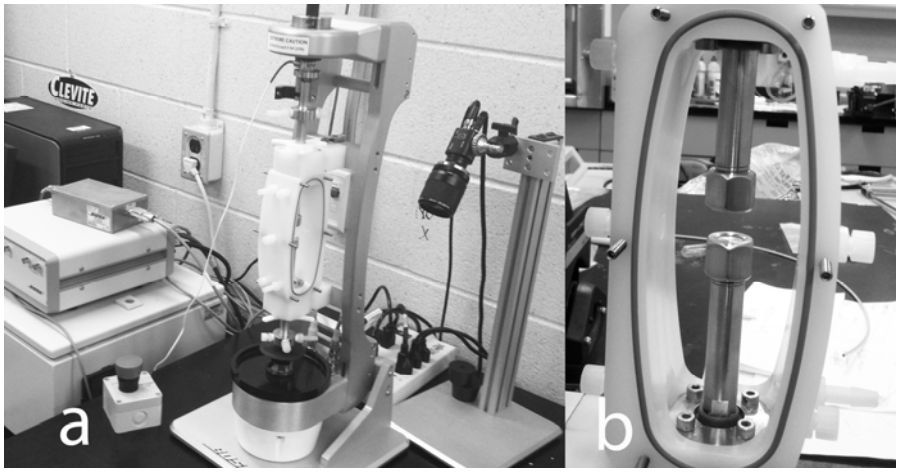


*Figure 2-1 ElectroForce® 3100 test instrument, a) the hardware of the instrument, b) the chamber structure*

The height, diameter, and weight of each specimen were measured in triplicate before mechanical tests. Then the specimen was placed between the two flat platens in the chamber installed on the frame, and the platens were released. The instrument was calibrated and adjusted through the WinTest® digital control system on a host computer. After calibration and adjustment, a ramp displacement generated by the WinTest® digital control system at a constant rate of 0.083 mm/s (5 cm/min) was applied on the specimen to provide a compressive force till a 20% strain (2.0 mm) was achieved. The data of load and displacement were collected and recorded by the WinTest® digital control system, and then the stress and strain were evaluated based on the following equations.

$$\sigma = \frac{F}{A} = \frac{4 \times F}{\pi D^2} \qquad \text{(Eq. (2.1))}$$

$$\varepsilon = \frac{\Delta l}{l_o} \qquad \text{(Eq. (2.2))}$$

where, $\sigma$ is the shear stress, $F$ is the load force applied on the specimen, $D$ is the diameter of the specimen (which was measured before the test), $\varepsilon$ is the shear strain, $\Delta l$ is the change in the length, and $l_0$ is the original length of the specimen before the test. All the measurements were done in triplicate, each time with a new specimen.

Then stress-strain curve was then plotted for the analysis on the mechanical properties (i.e. elastic modulus). From the stress-strain curve, the compressive elastic modulus ($E$) of this specimen was calculated from the following equation.

$$E = \frac{d\sigma}{d\varepsilon} \qquad \text{(Eq. (2.3))}$$

where, $d\sigma$ is the change in the shear stress and $d\varepsilon$ is the change in the shear strain. The compressive yield strength ($\sigma_Y$) was calculated by using 0.2% offset method on the stress-strain curve. Yield strength is the shear stress at which the permanent plastic deformation starts. As seen in Figure 2-2, the value of 0.2% offset yield strength is the intersection of the stress-strain curve and the line (called the offset) parallel to the elastic portion of the curve but with a strain offset of 0.002.

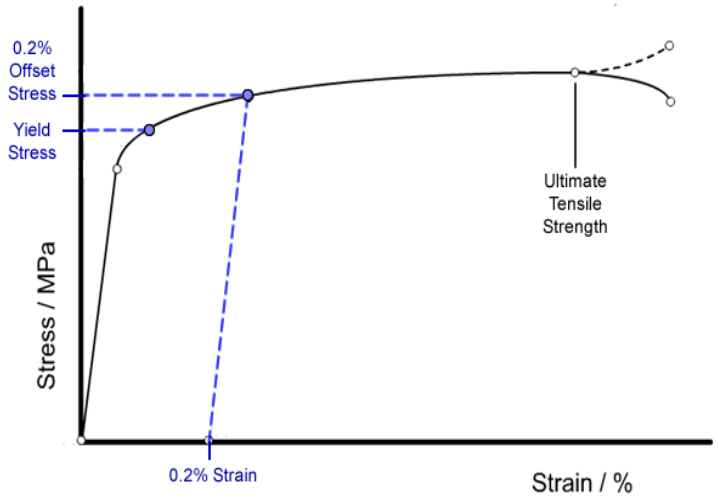


*Figure 2-2 0.2% Offset method todetermine the value of yield strength*

## 2.3 Experimental Results

The strain-stress curves were plotted based on the average values of three measurements at each testing point, shown in Figure 2-3. The figure shows the results obtained from both groups for all the four different concentration combinations. It is seen that the strain-stress curves of specimens of Group 1-1, 1-2, and 1-3 have similar character as typical ductile materials, i.e., the strain-

stress curve shows an approximate linear relationship before the shear stress reaches its yield point. The slope of this linear relationship gives the value of the elastic modulus or the Young's modulus. Generally speaking, the bigger the value is, the stiffer a material is. After the yield point, the curve decreased slightly because of the dislocation movements within the hydrogel structure. As the deformation continued, the stress increased until it reached the ultimate strength. Beyond this point, there would be an inflection in the curve, soon the fracture happened. The value of stress when the fracture happens gives the value of the breaking strength.

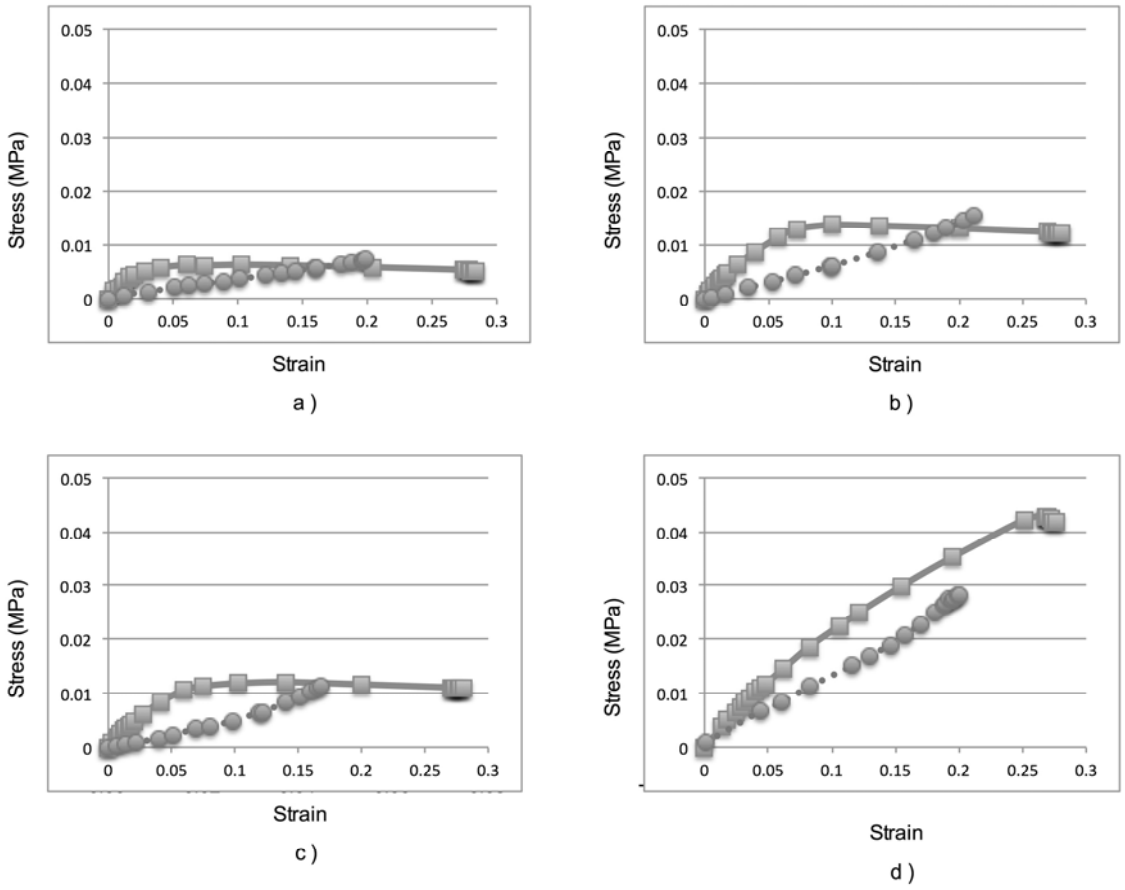


*Figure 2-3 Stain-Stress curve of alginate hydrogel, a ) 2% alginate and [Ca2+] 100mM solution, b ) 2% alginate and [Ca2+] 200mM solution, c ) 4% alginate and [Ca2+] 100mM solution, and d ) 4% alginate and [Ca2+] 200mM solution, post-treated group (■), control group (●), n=4*

For the specimens in Group 1-4, the strain-stress curve was linear and had no apparent yield point, which indicated that the specimens failed within the elastic deformation. The specimens in

Group 1-4 were more brittle, yet stronger, compared to those from the other groups. Because there is no yield point, there is no strain hardening either and the ultimate strength and breaking strength have the same value.

The results from control groups are shown in Figure 2-3. It is seen that all the strain and stress curves for all the specimens are linear and all specimens failed before reaching the yield point, indicating that all the specimens formed through this treatment were more brittle compared to those with post-fabrication treatment. Also it is suggested that the specimens formed by this method can bear more load, however, the strain value at which the specimens are broken was smaller than those obtained from the specimens with post-fabrication treatment.

### 2.4 Discussions

Alginate has been used in various tissue engineering applications, and its primary function is to provide mechanical integrity for scaffolding application, transmitting initial mechanical signals to the cells and developing tissue at the same time. Crosslinking is an widely used and effective way to stabilize 3D polymer networks in tissue engineering applications. Although covalent crosslinking has been widely used for the control of structural stability, mechanical properties, and hydrogel formation of many materials, the toxic crosslinkers and harsh gelation conditions make this approach not suitable for cell incorporation and encapsulation. Ionically crosslinking in this study employed nothing but calcium ion, which is a component of cytoplasm, with controlled gelation rate and properties for tissue engineering applications. The toxicity of calcium ions is studied and discussed in chapter 4.

Mechanical properties such as elastic modulus, yield strength, ultimate strength, and breaking strength were evaluated based on the strain-stress curve shown in Figure 2-3 in order to describe, compare and study the gels formed in different methods. The results obtained are listed in Table 2-1 and **Error! Reference source not found.**. For those made with post-fabrication treatment, student t-test showed that there is no significant difference on elastic modulus of the specimens from Group 1-1, Group 1-2 and Group 1-3, but the elastic modulus of Group 1-4 were significantly different from the ones in other groups ($p<0.05$). All these values are shown in Table 2-1. The yield strength of Group 1-1 was smaller than those of Group 1-2 and Group 1-3,

which suggested that the yield strength of alginate hydrogel increased with the increase of concentration of either alginate or calcium. The values of ultimate strength and breaking strength showed similar tendency. Furthermore, the specimens from Group 1-2 and Group 1-3 showed very similar mechanical properties, including elastic modulus, yield strength, ultimate strength, and breaking strength, even though the concentration of both reagents were different. The similarity between Group 1-2 and 1-3 might be because that the same influence of both reagents on the properties of hydrogel. Although the mechanical properties were very similar to each other, the chemical, biological properties and their toxicities might be different. And these properties will be discussed in later chapter of this thesis and is used as the criteria for choosing hydrogel forming factors for specific tissue engineering applications.

*Table 2-1Mechanical properties of hydrogel specimens made with post-fabrication treatment*

| | Group 1-1 | Group 1-2 | Group 1-3 | Group 1-4 |
|---|---|---|---|---|
| Gelling Temperature | 25℃ | | | |
| Gelling Time | 6 hoursin mold + 24 hours in 100mM [$Ca^{2+}$] | | | |
| Test Temperature | 20℃ | | | |
| Strain Rate | 0.083mm/s | | | |
| Strain | 0.3 | | | |
| Elastic Modulus (MPa) | 192.7 ± 16.7 | 176.9 ± 7.6 | 178.6 ± 7.6 | 146.5 ± 3.9 |
| Yield Strength (kPa) | 5.12 ± 0.3 | 12.9 ± 1.5 | 10.0 ± 0.7 | - |
| Ultimate Strength (kPa) | 6.2 ± 0.8 | 13.6 ± 1.1 | 12.1 ± 0.5 | 42 ± 3.4 |
| Breaking Strength (kPa) | 5.09 ± 1.3 | 12.2 ± 0.7 | 11.1 ± 0.9 | 42 ± 3.4 |

For those in the control groups, one-way analysis of variance (ANOVA) and student t-test showed significant difference on both elastic modulus and breaking strength among all groups ($p<0.05$). It is observed from Table 2-2 that the value of either elastic modulus or breaking strength nearly doubled as the concentration of alginate increased from 2% to 4%, and the values doubled when the concentration of calcium increased from 100mM to 200mM. These results showed that both elastic modulus and breaking strength increased with the increasing concentration of either alginate or calcium, however, the effect of the concentration of calcium

seems to be more profound than the effect of alginate. The result also showed that the higher the concentration of both reagents is the stronger the hydrogel specimen is. Like the specimens in the first treatment group, the mechanical properties of those from Group 2-2 and 2-3 are not much different from each other.

*Table 2-2 Mechanical properties of hydrogel specimens made without post-fabrication treatment*

| | Group 2-1 | Group 2-2 | Group 2-3 | Group 2-4 |
|---|---|---|---|---|
| Gelling Temperature | 25℃ | | | |
| Gelling Time | 24 hours | | | |
| Test Temperature | 20℃ | | | |
| Strain Rate | 0.083mm/s | | | |
| Strain | 0.3 | | | |
| Elastic Modulus (MPa) | 35 ± 0.4 | 70.7 ± 0.8 | 66.3 ± 0.3 | 139 ± 3.4 |
| Yield Strength (kPa) | None | | | |
| Ultimate Strength (kPa) | 7.2 ± 1.2 | 15.3 ± 1.4 | 11.2 ± 1.0 | 28.3 ± 1.5 |
| Breaking Stress (kPa) | 7.2 ± 1.2 | 15.3 ± 1.4 | 11.2 ± 1.0 | 28.3 ± 1.5 |

Also, student t-test showed that the mechanical properties of same reagent concentration combination in different treatment groups, comparing Group 1-1 with 2-1, Group 1-2 with 2-2, Group 1-3 with 2-3, were very different ($P<0.01$). The difference in the mechanical properties between the specimens formed from the aforementioned two different treatments is likely due to the difference of the degree of crosslinking of the specimens. The degree of the crosslinking is influenced by the concentration of both reagents, gelation time, and type of alginate. The concentration of the reagents influences the mechanical properties of the formed hydrogel in a very direct way. With increasing concentration of either reagent, the gelation rate increases. This, as a result, leads to formation of a non-uniform gel structure, thus weakening the mechanical properties of the formed hydrogel.

On the other hand, gelation time has a significantly impact on the mechanical properties of alginate hydrogel, as it has been shown through the post-fabrication treatment in this study. The mechanical properties of hydrogels from both post-fabrication treated group and control group

vary in a large range. However, the hydrogels formed with a post-fabrication treatment generally had greater values of elastic modulus than those formed without the treatment. This finding suggests that the hydrogels can be strengthened through a post-fabrication-treatment, i.e., immersing formed hydrogel in a calcium chloride solution with relatively low concentration for longer time in order to strengthen the hydrogel. Also, because the experiment was aiming to gain knowledge for fabrication of scaffold using in spinal cord regeneration, the results obtained from mechanical test were compared with mechanical properties of spinal cord. And it's noticed that the mechanical properties of the samples in post-fabrication treated groups (Table 2-1) were close to real spinal cord (elastic modulus 1.4 MPa, Yield Strength 0.089 MPa, ultimate strength 0.66 MPa) [144, 145]. This also showed that post-fabrication treatment had a great potential of charactering the mechanical properties for desired tissue engineering application.

## 2.4 Conclusions

The work presented in this chapter is a study on the influence of process parameters of hydrogel formation on the mechanical properties of the hydrogel formed. The results demonstrate that the mechanical properties of the hydrogel can be controlled by the concentrations of alginate and calcium chloride. It is also demonstrated that the gelation time has a significantly impact on the mechanical properties of alginate hydrogel, and that the hydrogel formed by mixing solutions of both reagents with higher concentration together first and then being strengthened by immersion in calcium solution with lower concentration can increase the elastic modulus of hydrogel. This result suggested that the hydrogels could be strengthened through a post-fabrication-treatment, i.e., immersing the hydrogel in a calcium chloride solution with relatively low concentration. The mechanical properties of the hydrogel scaffold can be controlled and modified by the concentrations of both crosslink reagents and the gelation time in the post-fabrication-treatment.

# Chapter 3 SCAFFOLD FABRICATION

## 3.1Introduction

Dispensing-based scaffold fabrication is one of the most promising scaffold fabrication techniques due to its fast and efficient material processing. Previous studies have shown the structure of fabricated scaffold can be affected by various fabrication process parameters. This chapter presents an experimental study on the influence of some of critical parameters in the fabrication process, including the applied pneumatic pressure, the diameter of nozzle used, the concentration of alginate solution, and the movement speed of the dispenser. The optimal combination of these parameters that produced the desired hydrogel struts was obtained through experimental study. Eventually, 3D hydrogel scaffolds were fabricated using the dispensing method based on the selected parameters.

## 3.2 Materials and Methods

### 3.2.1Preparation of Alginate and Calcium Solutions

The aqueous solutions for scaffold fabrication were prepared from low viscosity sodium alginate (Sigma, St. Louis, MO) with molecular weight range 12,000~80,000 Da (mannuronic acid 61% and guluronic acid 39%) in deionized water, at concentrations of 2% to 4% (w/v).

Calcium chloride (Sigma, St. Louis, MO) was dissolved in deionized water at a concentration of 100 mM/L, which was used as the crosslinker to gel the sodium alginate aqueous solution.

### 3.2.2 Scaffold Fabrication System and Process

The dispensing-based system for scaffold fabrication employed in this study was constructed and adapted from a typical commercial fluid dispensing system (C-720M, Asymtek, USA). As shown in Figure 3-1 (a), the system consists of two dispensers, a pneumatic dispenser and an motor-driven one, mounted on a three-axis positioning system, a platform to support the scaffold being fabricated, a host personal computer, and three controllers interfaced with the host

computer for controlling of dispensers, positions, and temperature of different components. This system has unique features compared to existing scaffold fabrication systems such as the use of two different types of dispensers, and the integration of the temperature control of both dispensers and the platform. These features allow for delivering various scaffold materials, viable cells, growth factors and/or other bioactive compounds at the same time. A close-up view of the pneumatic dispenser applied in this study is shown in Figure 3-1 (b). The flow rate of this dispenser can be controlled through adjusting the pressure of compressed air.

The fabrication process of 3D scaffold proceeded as follows. First, alginate solution was loaded into a syringe and then the syringe was installed on the dispensing system. The air pressures were set at the values as determined in the experiments presented later. Under the action of compressed air, the alginate solution loaded in the syringe was extruded, through a needle, into the reservoir containing calcium chloride solution for crosslinking, while the dispenser was brought to move at a defined speed in the X- direction. Straight lines of alginate hydrogel, with a space of 500μm between two lines, were formed for the first layer. Once the first layer was formed, the needle was lifted up and then brought to move along the Y- direction at the same speed to form the second layer. In this manner, a two-layer scaffold was fabricated at room temperature.

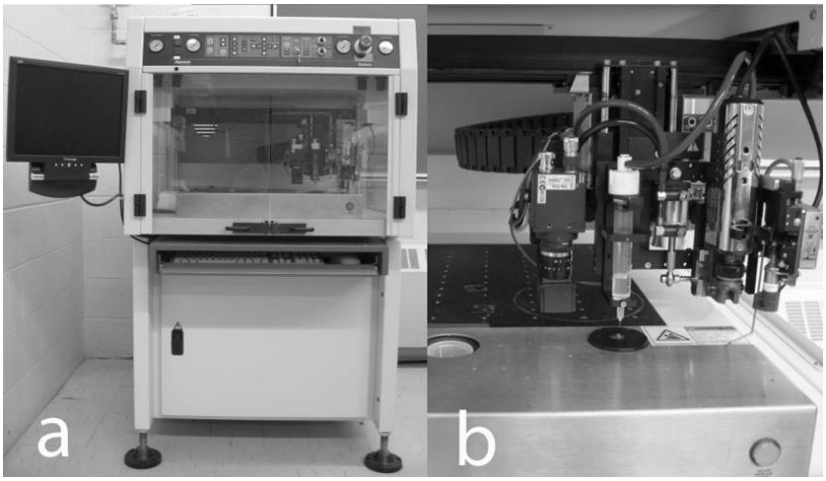


*Figure 3-1 Scaffold fabrication system, a) whole system, and b) close-up view of working space.*

### 3.2.3 Scaffold Geometry Characterization

The cross-section profile of the scaffold struts is an important parameter to characterize in fabrication of scaffolds. In this study, the strut profile was measured using a non-contact 3D laser scanning profilometer (Vantage 50, Cyber Tech., USA). This system mainly consists of a laser sensor, a base, and a host computer for data acquisition and analysis, as shown in Figure 3-2 (a). This system has a wide range of measurement and a resolution up to 0.01 μm. The confocal laser sensor can also produce a 3D line-scan capability with 1.1mm width and 2 μm lateral resolution. To illustrate the application of this system in profile measurement, the cross-section profiles of dispensed hydrogel struts were measured as shown in Figure 3-2 (b). The diameters of these struts were calculated as approximately the average of the values in both vertical and horizontal directions.

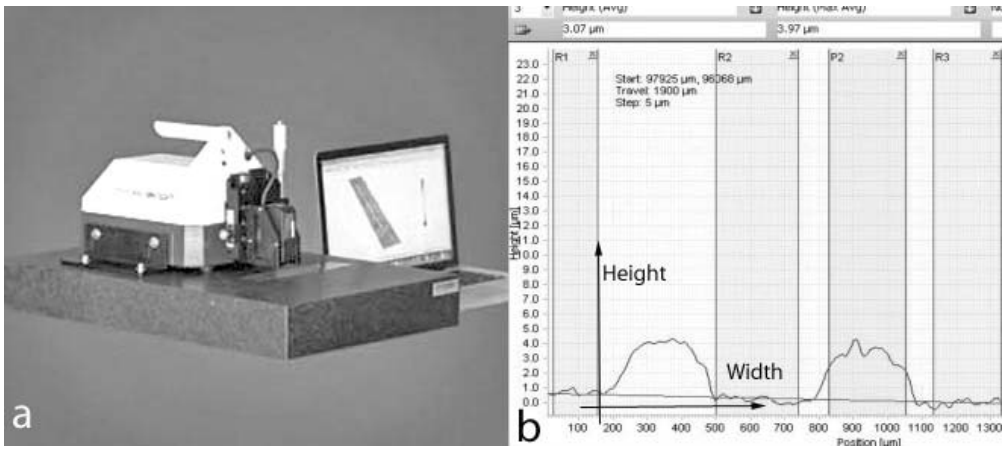


*Figure 3-2 a) Cyber scan vantage 50 profiling system, and b) typical cross-sectional profile measured.*

## 3.3 Results

### 3.3.1 Experimental Investigation into Fabrication Process

In the scaffold fabrication process, the process parameters such as such as nozzle diameter, applied air pressure, and the moving speed of the dispenser can significantly affect strut diameters of fabricated scaffolds. This section presents an experimental investigation into this influence, which forms the basis to rigorously select and determine the process parameters for subsequent scaffold fabrication. Both 2% and 4% (w/v) alginate solutions were used. In the experiment, struts were printed by the dispensing system with nozzles of internal diameter of 100

μm, 250 μm, and 410 μm nozzles under the pressure of 2 psi, 5 psi, 10 psi, and 20 psi. The moving speed of dispenser was varied from 30 mm/s to 55 mm/s in 5 mm/s increments.

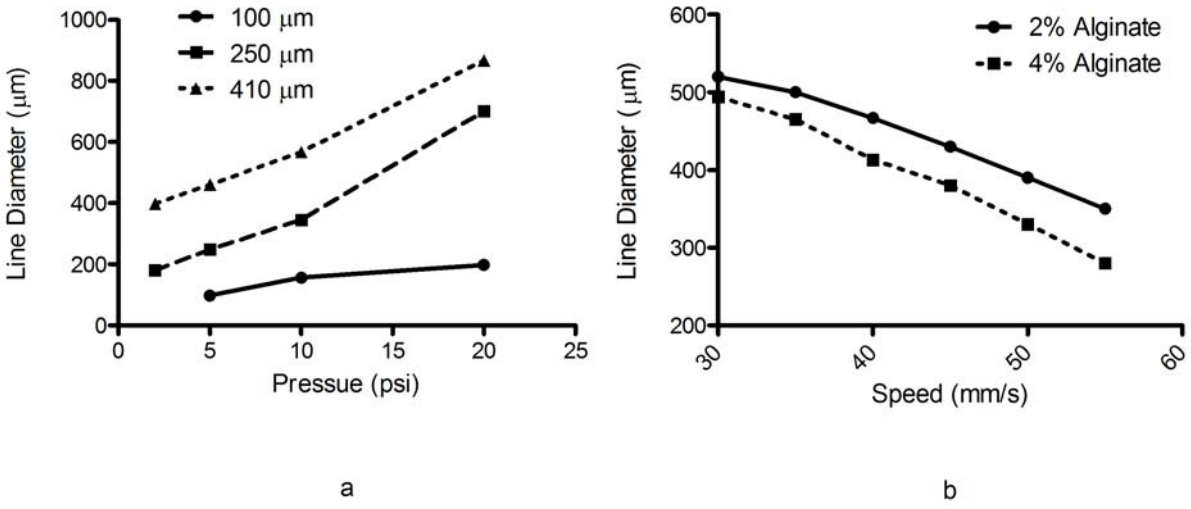


*Figure 3-3 Influence of process parameters on the strut diameter: a) air pressure (for 4% (w/v) alginate solutions and b) moving speed of dispenser (with an air pressure of 5 psi).*

Specifically, the influence of applied air pressure was investigated by printing struts with 4% (w/v) alginate solution using 100 μm, 250 μm, and 410 μm nozzles at 2 psi, 5 psi, 10 psi, and 20 psi. The results obtained are shown in Figure 3-3 (a). It is seen that the diameter of the hydrogel line increased with the value of air pressure and the nozzle diameters. Compared to the use of 250 μm and 410 μm nozzles, the influence of air pressure on the diameter of the hydrogel lines is much less significant if a 100 μm nozzle was used [146].

Both 2% and 4% (w/v) alginate solution were extruded out with 250 μm at 5 psi printing pressure in order to study the influence of moving speed of dispenser. The results are shown in Figure 3-3 (b). It is seen that the diameter of printed hydrogel strut is not constant, but decrease more than 50% for both concentrations if the speed increase from 30 mm/s to 55 mm/s. This suggests that the moving speed of dispenser is an important parameter for controlling the diameter of hydrogel strut besides the air pressure and the nozzle diameters, as shown in Figure 3-3 (a). Also, the results suggest that the diameter of hydrogel strut can be affected by the concentration of alginate in the solution.

The alginate solution was also extruded into 100 mM calcium chloride. In the experiments, nozzle with diameters of 100 μm, 250 μm, and 410 μm, were used for dispensing, and the applied air pressure varied from 2 psi to 20 psi in 2 psi increments; and the dispenser was brought to move horizontally at a speed varying from 5 mm/s to 65 mm/s in 5 mm/s increments. A trial and error method was used to find the dispensing conditions such that the diameter of struts has the same value as the nozzle diameter. In such struts, neither compression nor tension stress exist. Table 3-1 lists the dispensing conditions for the strut diameters that are near to the nozzle diameters. All the measurements were done in triplicate.

*Table 3-1 Dispensing conditions and strut diameters*

| Concentration (w/v) | Air Pressure (psi) | Nozzle Diameter (μm) | Speed of dispenser (mm/s) | Diameter of Hydrogel (μm) |
|---|---|---|---|---|
| 2% | 10 | 100 | 25 | 156 |
| | | | 35 | 98 |
| | 2 | 250 | 35 | 279 |
| | | | 45 | 248 |
| 4% | 2 | 410 | 50 | 573 |
| | | | 55 | 456 |
| | 20 | 100 | 25 | 198 |
| | | | 30 | 130 |
| | 6 | 250 | 35 | 261 |
| | | | 45 | 212 |
| | 2 | 410 | 45 | 494 |
| | | | 50 | 470 |

### 3.3.2 Fabrication of Hydrogel Scaffold

Using the process parameters obtained above, a 3D porous structure hydrogel scaffold was fabricated. Specifically, 10 mL of 2% (w/v) alginate solution was loaded into a syringe with a needle of 250 μm diameter connected to it. The air pressure value was set as 2 psi based on the results presented in Table 3-1. With the needle moving at a speed of 35 mm/s, the alginate solutions were extruded into the reservoir of calcium chloride solution to crosslink while the dispenser was moving at a constant speed in the X- direction to form a straight line of alginate hydrogel. The first layer was fabricated with a space of 500 μm between struts, and then the

needle was lifted up 0.6 mm and brought to move along the Y- direction for the second layer. The scaffold was fabricated layer by layer. The scaffold formed is shown in Figure 3-4.

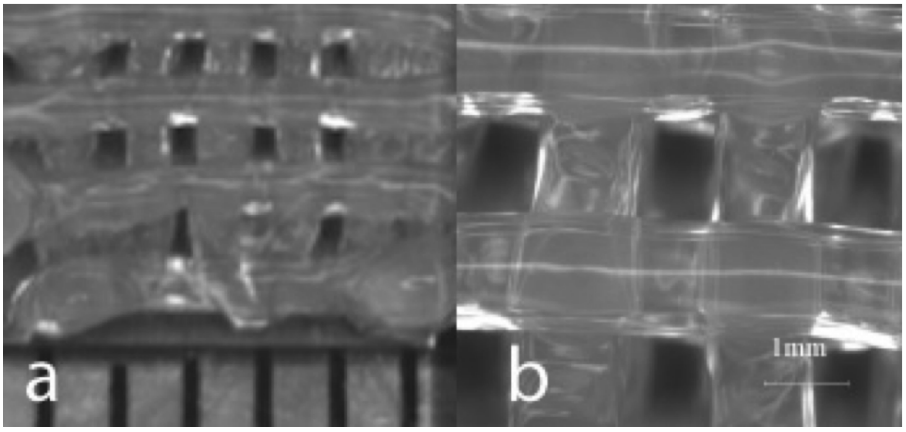


*Figure 3-4 Three-dimensional pore structural hydrogel scaffold (a) top view, and (b) close-up view*

The fabricated hydrogel scaffold had a multilayer structure, and was able to be manipulated by means of tweezers, which provides the possibility for future employment in a clinical setting.

### 3.4 Discussions

The results showed that the diameter of fabricated hydrogel strut were influenced by the value of air pressure, nozzle size, and the moving speed of the nozzle. The relationship between all these factors can be explained by this equation developed in literatures [147]:

$$D = \sqrt{\frac{4Q}{\pi v}} \qquad \text{(Eq. (3.1))}$$

$$Q = \frac{\pi r^4}{8\eta}\frac{dP}{dz} \qquad \text{(Eq.(3.2))}$$

where, $D$ is the diameter of fabricated hydrogel strut, $Q$ is the flow rate, $v$ is the moving speed of nozzle, $\frac{dP}{dz}$ is pressure gradient, and $\eta$ is the viscosity of employed solution. And the results from the experiments affirmed the relationship described by these equations. However, another crucial factor for this fabrication process which has been noticed in the experiments was

not included in the equations, that is, the gap distance between the nozzle and the surface of calcium solution.

In according to the value of flow rate, there are two modes of polymer deposition; the extrusion mode and the droplet mode, as shown in Figure 3.5. In both modes, the material is extruded out of the nozzle tip under an applied pressure. In the extrusion mode, the material was laid down in the form of line structures in order to create the desired model by moving the nozzle tip over a substrate in desired path. And, a 3D structure can be developed by repeating this process layer by layer. While in droplet mode, the material is deposited in the form of droplets. A structured layer can be formed by depositing multiple droplets in desired locations on a substrate. Similarly, this process can be repeated to fabricate a 3D structure.

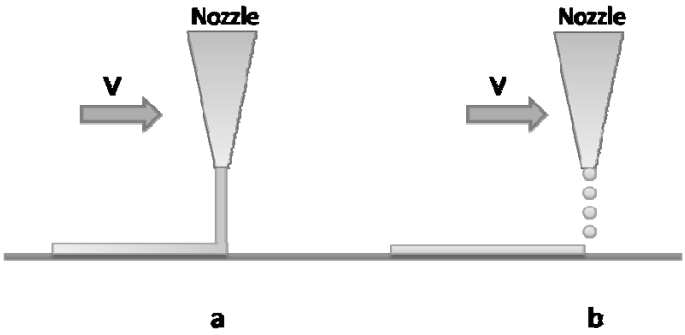


*Figure 3.5 Schematic of polymer deposition: a) extrusion mode, b) droplet mode*

Because of the involvement of calcium aqueous solution, surface tension between water and employed material has been introduced into this dispensing process. Because that employed material tends to assemble into the shape of spherical cap under the influence of surface tension, the hydrogel line will be curved or break into pieces in the fabrication process. Also, the pattern fabricated in this process tended to float on the surface of calcium solution because of the effect of surface tension. Although the influence of surface tension cannot be neglected in this micro-sized tissue engineering context, it can be minimized by adjusting the distance between nozzle and the surface of aqueous solution. When the gap is adjusted to the value at which allows extruded material form a bridge between the nozzle and the surface of calcium reservoir, the material will form a straight line at the proper moving speed under the effect of viscosity in both aforementioned dispensing modes. The expanding effect of hydrogel will also be minimized when the gap is suitable because of the instant solution-gel formation.

### 3.4 Conclusions

In this chapter, experiments were conducted to investigate the influence of process parameters on scaffold fabrication. The results obtained show that the air pressure, the dispensing nozzle size, and the concentration of alginate solution can affect the diameter of scaffold struts. The results also show that the horizontal movement speed of dispenser is critical to the control of the diameter of hydrogel struts. With given pneumatic pressure, nozzle size, and alginate concentration, the movement speeds of the dispenser were determined experimentally such that the diameters of the hydrogel struts obtained were close to the diameters of the nozzles used. Eventually, such parameters as the air pressure, nozzle size, alginate solution concentration, and the horizontal speed were rigorously selected for the scaffold fabrication and 3D hydrogel scaffolds were successfully fabricated.

# Chapter 4 CELL SURVIVAL AND PROLIFERATION IN CROSSLINKING PROCESS

## 4.1 Introduction

Incorporating living cells into tissue-engineered scaffolds is an attractive and promising research topic in biofabrication. Although there are many studies on a variety of biofabrication techniques, the maintenance of cell function and structure and protection from damage is still a challenging topic. Cell damage can be caused by toxic solvent and its residual in the solvent casting process and/or by the sublimation of water by, for example, lyophilization. For the milder dispensing based RP technique concerned in this present work, it is mainly believed that cell damage can be caused by mechanical forces, such as shear stress and hydrostatic pressure, to which cells are exposed during the fabrication process [125, 148]. This chapter presents an investigation into another potential influence on cell survival by the concentration of calcium chloride solution used for crosslinking alginate during the biofabrication process. After fabrication, with the degradation of alginate hydrogel, calcium ions may be released from the crosslinking bond, thus potentially further affecting such cell functions such as survival and proliferation. An investigation into this influence is also included in this chapter. Finally, this chapter also looks at the influence of cells density on cell survival and solution viscosity.

## 4.2 Materials and Methods

### 4.2.1 Culture for Schwann Cells

Schwann cell line (RSCs 96, CRL- 2765) were purchased from ATCC (American Type Culture Collection ATCC, Manassas, VA), at passage 9. Schwann cells were harvested between passage number 9 and 13 for all the experiments in this study. The cells were maintained in standard Dulbecco's Modified Eagle Medium (DMEM) supplemented with 10% fetal bovine serum (FBS) (Invitrogen Co, Carlsbad, Calif, CA, USA). The cells were grown in 10 cm tissue culture dish at 37°C in a 5% $CO_2$ relatively humidified environment, and the media were changed every other day. At 100 percent confluency, cells were washed with 1 mL 0.25% Trypsin/EDTA (Invitrogen)

for 1 min to detach the cells from the dish. Then cell suspensions were delivered into a sterile 15 mL falcon tube and centrifuged at 800 rpm in a centrifuge for 5 min. Eventually, the cells were counted and resuspended with fresh media to the desired cell density.

### 4.2.2 Alginate Preparation and Encapsulation of Schwann Cells

The alginate solution was prepared from low viscosity sodium alginate (Sigma, St. Louis, MO, USA), with molecular weight range 12,000~80,000 Da (mannuronic acid 61% and guluronic acid 39%), and DMEM solution with 10% FBS, at a concentration of 2% or 4%,. Schwann cell suspension, as prepared above, was added to alginate solution at various volume ratios. The cell-alginate mixture was placed in the wells of a 96-well tissue culture plate with a volume of 100 μL per well.

Calcium chloride (Sigma, St. Louis, MO) was dissolved in deionized water at concentrations of 100 mM, 500 mM, or 1 M, and then added into the wells to crosslink the alginate and, form hydrogel. Thirty min later, the hydrogels were rinsed three times, submerged in DMEM, and incubated at 37 °C in a 5% CO2 humidified environment. The cell media were refreshed every other day. As the control group, Schwann cells were also cultured in DMEM solution with 10% FBS in the 96-well plates with no additional calcium chloride..

### 4.2.3 MTT Assay for Cell Damage

The MTT assay was used to measure cell survival and proliferation rate in this study. MTT (3-(4,5-Dimethylthiazol-2-yl)-2,5-diphenyltetrazolium bromide, a yellow tetrazole) is reduced to purple formazan in living cells. A solubilization solution (usually either dimethyl sulfoxide, an acidified ethanol solution, or a solution of the detergent sodium dodecyl sulfate in diluted hydrochloric acid) was added to dissolve the insoluble purple formazan product into a colored solution. The absorbance of this colored solution can be measured at a certain wavelength (usually between 500 and 600 nm) using a spectrophotometer [149]. In this study, MTT was dissolved in PBS to obtain a stock solution with a concentration of 5 mg/mL. The stock solution must be filter sterilized after mixing. A solution of 4 mM HCl, 0.1% Nondet P-40 (NP40) in isopropanol was used as the MTT solvent.

Schwann cells suspended in alginate gel were cultured in a 3D condition. Hydrogels made from 100μL alginate solution with a concentration of 2% (w/v) or 4% (w/v), were placed in the wells

of a 96-well plate. Two dimensional (2D) monolayer cultures were 100 μL cell suspension with a density of $2\times10^5$ cells/mL in each well of 96-well plates of non-encapsulated Schwann cells with treatments of calcium chloride solution, with a concentration of 100 mM, 500 mM, and 1 M, for 5 min, 10 min, and 30 min. After treatments, the cells were washed three times with DMEM and then 20 μL of MTT stock solution was added into each well of both gel-suspended and non-encapsulated cells. After three and half hours incubation in an incubator at a condition of 37°C 0.5% $CO_2$, all the media were carefully removed and then 150 μL MTT solvent was added into each well. The 96-well plate was then covered with aluminum foil and agitated on an orbital shaker for 15 min, and the absorbance at 590 nm was measured with a reference filter of 620 nm. A SpectrMax 250 Monochromatic spectrophotometer (GMI Inc, Minnesota, USA) was used to measure the absorbance reading. The monochromatic based system provides a precise wavelength, 250-850 nm in 1 nm wavelengths increments. Optical density (OD) can be determined by means of an endpoint reading or a kinetic analysis can be used to measure the rate of optical density change per minute (OD/min) [150].

### 4.2.4 MTT Assay for Proliferation

Both gel-suspended and non-encapsulated cells were immersed in DMEM (10% fetal bovine serum) with or without the treatments of calcium chloride solution. MTT stock solution was added in the cell cultures and the amount of formazan produced was assessed by spectrophotometer as described above. Measurements were made at 6, 12, 24, 48, 72, and 96 hours for the comparison of proliferation of Schwann cells. In this study, the densities of cells were $2\times10^5$ cells/mL, $6\times10^5$ cells/mL, or $8.5\times10^5$ cells/mL, for investigating the influence of cell density on cell proliferation.

### 4.2.5 Rheological Study

Alginate solutions with a concentration of 2% (w/v) or 4% (w/v), were prepared with DMEM solution. Schwann cells were suspended in alginate solution at a density of $4\times10^5$ cells/mL, $8\times10^5$ cells/mL, or $4\times10^6$ cells/mL. The rheological properties of the cell-alginate mixture were measured by using a rheometer (Brookfield DV-III+ Programmable rheometer, Brookfield, Middleboro, MA). This rheometer has a cone and plate structure with the shear rate being controlled via programming. The rheometer also provides the ability to collect and record the

data during the rheological tests In the present study, a CP 41 spindle was selected for use, which requires samples of 2 mL alginate solution or its mixture with Schwann cells. After zeroing and calibrating the rheometer, the viscosity was measured at varying shear rates via the control of the spindle rotation speed sweeping from 10 RPM to 250 RPM in 30 RPM increments. All the measurements were repeated five times.

## 4.3 Results

### 4.3.1 Cell Survival and Proliferation in Cell Culture

Schwann cells were cultured in the wells of a 96 well plate in DMEM/FBS media at a density of $2\times10^5$ cells/mL. Calcium chloride solution with a calcium concentration of 100mM, 500mM, and 1 M, were added into cell cultures. At different time periods of 5, 10, 30 minutes, the solution in each well were carefully removed, only leaving the Schwann cells attached to the well. Attached Schwann cells were washed three times with DMEM, covered again with medium, and then incubated at 37 °C in a 5% CO2 humidified environment for a time period of 6 or 24 hours. By doing so, the cell cultures were exposed to different calcium concentration for varying time periods, which is assumed to affect cell survival and proliferation afterwards. Two control groups were used in the experiments. One group was treated with DMEM with no added calcium chloride (negative control), to which the cell number and proliferation of other groups are compared; and other group was treated with distilled water for 30 min, in which cells were mainly damaged by the osmotic pressure (positive control) in order to calibrate the absorbance reading and calculate the number of living cells.

The absorbance readings of living cells were measured by means of the spectrophotometer mentioned previously. For the characterization of cell survival and proliferation, an index of the relative cell number was used in the present study. The relative cell number is evaluated from the spectrophotometer absorbance reading based on the linear relationship between the relative cell number and the absorbance readings. To establish the linear relationship, the values of the absorbance readings of the positive control group (the number of living cell is zero) and a group with 2000 living cells were used. Through this relationship, all absorbance readings were converted into the relative numbers of cells. All the relative numbers of living cells were calculated through this method in this chapter unless specified.

Figure 4-1 shows the numbers of living cells measured at 6 hours after the cell cultures were exposed to the calcium environment, as compared to those in control groups. It is seen that the exposure of cells to the calcium environment can cause significant loss in living cells, about half of which were damaged even within 5 min exposure, compared to the DMEM group. However, the difference due to the calcium concentration and exposure time on cell survival is not significant.

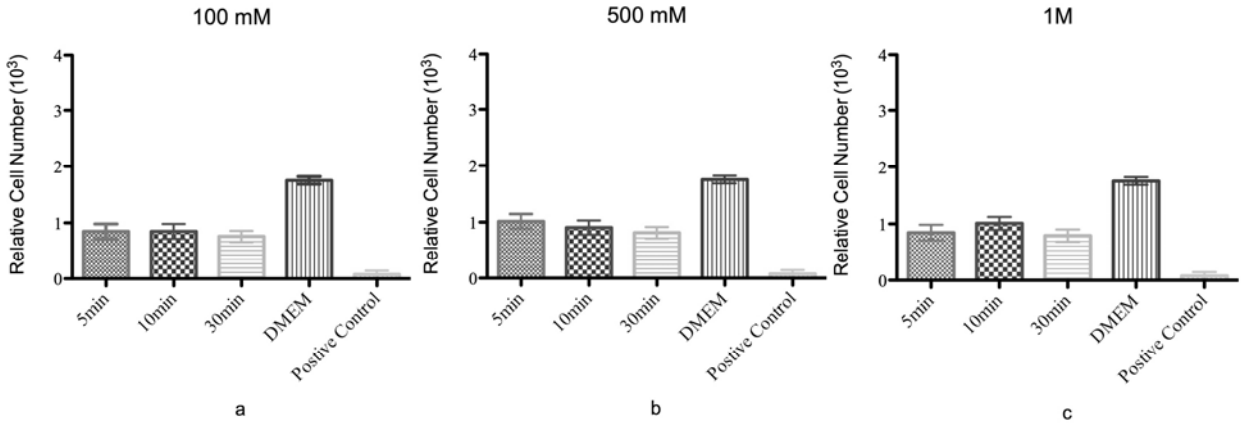


*Figure 4-1 Number of living cells 6 hours after calcium solution treatment with concentration of a) [$Ca^{2+}$] 100mM, b) [$Ca^{2+}$] 500mM, and c) [$Ca^{2+}$] 1M, n=8, P<0.05*

Figure 4-2 shows the numbers of living cells measured at 24 hours after the cell cultures were exposed to the calcium environment, as compared to those in control groups. As observed, the number of living cells in the cultures exposed to 1M calcium concentration continued decreasing after 24 hours compared to the number in 6 hours, which indicated that high calcium concentration could lead to permanent cell damage. While the statistic analysis showed that the number of living cells in lower calcium concentration, especially for those treated with 0.1M calcium solution, significantly increased after 24 hours compared to their values in 6 hours ($P<0.05$). Although the proliferation rates of the cells treated with the lower calcium concentration were lower than those in the DMEM control group, the increasing number of living cells showed that the surviving cells were functionally active. The result also showed that the exposure time has a negative influence on the cell survival, which suggests the time period of using calcium chloride solution for crosslinking in the fabrication process must be limited.

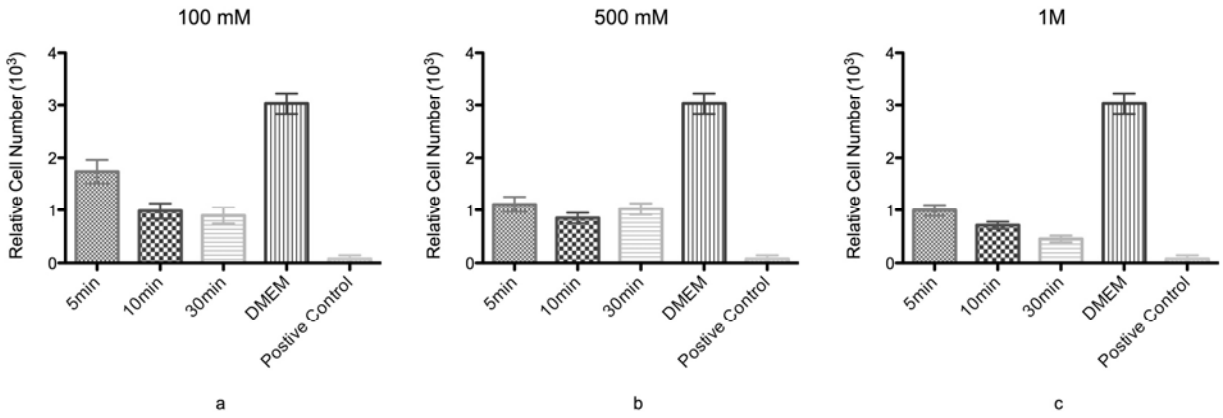


*Figure 4-2 Number of living cells 24 hours after calcium solution treatment with concentration of a) [Ca2+] 100mM, b) [Ca2+] 500mM, and c) [Ca2+] 1M, n=8, P<0.05*

### 4.3.2 Cell Survival and Proliferation in Cell- Alginate hydrogel

It has been reported that the cells behave differently if they are cultured in 3D instead of 2D environment. Thus, to study cell survival and proliferation in 3D calcium environment or engineered constructs is essential. This section presents the examination results of cell survival and proliferation in cell-alginate hydrogel that were crosslinked by means of calcium chloride solution.

The cell density was set to $4\times10^5$ cells/mL in all the experiments presented in this section. Figure 4-3 shows the numbers of living cells measured at 24 hours after the formation of hydrogel from the cell-alginate cultures with alginate concentrations of 2% or 4% (w/v), by using calcium chloride solution for crosslinking, as compared to those in control groups (i.e., cells cultured in DMEM medium alone). It is seen that the numbers of living cells in both 2% and 4% alginate solutions were lower than those in the control group. However, these alginate-suspended cells showed a greater survival rate than cells without alginate with the same calcium treatment (Figure 4-2). This suggests that the use of alginate provides a favorable environment for cell survival and proliferation if the cells are exposed to calcium.

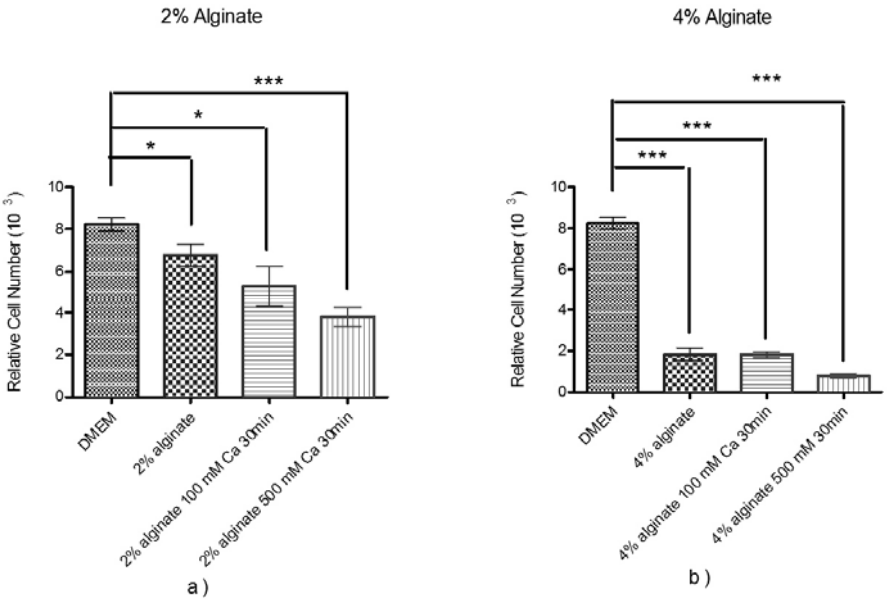


*Figure 4-3 Number of living cells 24 hours after calcium solution treatment in a) 2% alginate solution and b) 4% alginate solution, ANOVA, n=8, P<0.05, Student t-Test, * represents P<0.05, ** represents P<0.01, *** represents P<0.001*

The results in Figure 4-3 shows a very low survival rate in 4% alginate solution as compared in 2% alginate solution. This is possibly due to the reversible inhibition effect of 4% alginate solution on cells as previously reported [87]. The results obtained suggests that low (i.e., 2%) concentration alginate solution is more suitable for cell encapsulation in engineering tissue scaffolds, as compared to high (i.e., 4%) concentration alginate solution.

Figure 4-4 shows the results, as examined within a longer time period of 100 hours, of cell proliferation both in DMEM and in alginate solutions with varying cell densities. The proliferation curve of cells in DMEM with cell density of $2\times10^5$ cells/mL was used as the control group in these experiments. As observed, the proliferations of cells in both DMEM and alginate solution were influenced by cell density. The proliferation rate increased with the cell density, suggesting that cell density has a positive influence on cell proliferation. This might due to increased cell-cell chemical and biological stimulation for increasing the proliferation rate. When the cells were cultured at the same density, the proliferation rate of the cells in alginate solution was slower compared to those in DMEM; while the proliferation rate in 4% alginate was slower

than the one in 2% alginate. This showed that the concentration of alginate had a negative influence on cell proliferation. The reason might be that the alginate slows down the absorption and exchanging of ions and proteins in the extracellular environment (as suggested in Figure 4-4 (d)), the encapsulated cells were more rounded in alginate and perhaps could not form regular cell-cell interactions as they did in DMEM alone. With increased cell density, the contact between cells increased thus the proliferation rate was higher. The number of cells in DMEM, shown in Figure 4-4. (a), decreased after certain time periods, depending on the cell density; this was due to the limited space of the wells of a 96-well plate where those cells were cultured. When cell number reached a certain level, the well would be overpopulated, leading to an unhealthy condition, cessation of cell proliferation and eventually the death of cells. The result of this study suggested that high cell density and low (i.e., 2%) alginate concentration were more suitable for further studies.

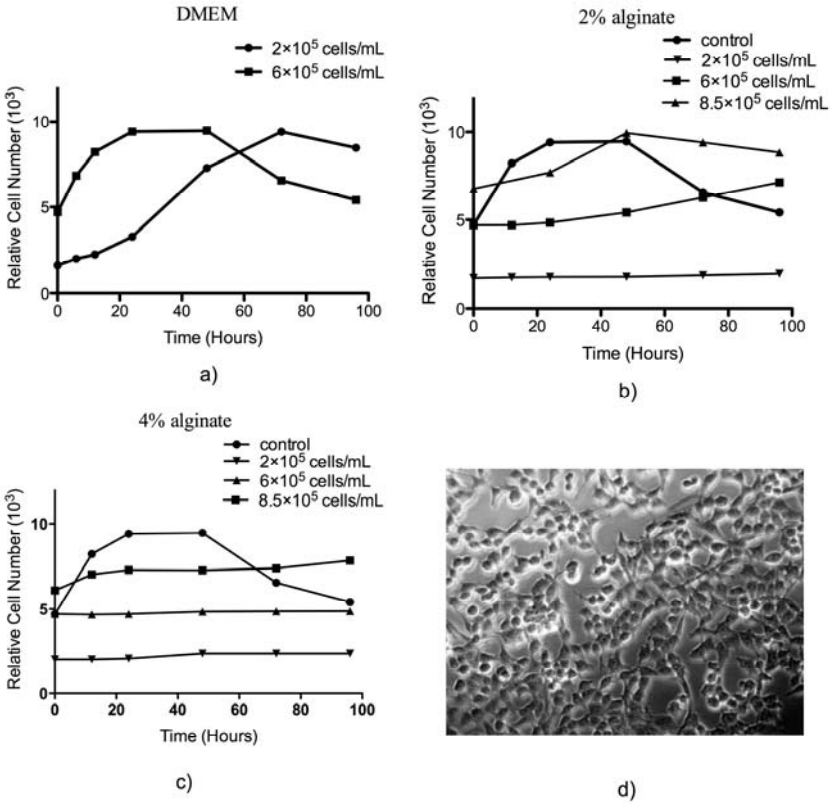


*Figure 4-4 Influence of cell density on alginate encapsulated cells: a) Schwann cells in DMEM, b) Schwann cells in 2% alginate, $6\times10^5$ cells/mL in DMEM as control, c) Schwann cells in 4% alginate, $6\times10^5$ cells/mL in DMEM as control, and d) optical image of Schwann cells in 2% alginate*

Cell proliferation was also measured in hydrogels formed by both 2% and 4% (w/v) alginate solution by MTT assay. The results are shown in Figure 4-5. Alginate solutions were mixed with Schwann cells at the density of $8.5\times10^5$ cells/mL. Alginate cell mixtures were crosslinked with calcium solution at concentration of 100 mM or 500 mM for 30 mins to form hydrogels and then the hydrogels were rinsed with DMEM solution three times. Then all the hydrogels as well as cell-alginate mixtures which were used as the control group were moved into the wells of a 96-well plate, each covered with 100 μL medium and incubated at a condition of 37°C 0.5% $CO_2$. It can be observed that cells in both 2% and 4% (w/v) alginate hydrogels showed proliferation. For those encapsulated in 2% alginate hydrogels (Figure 4-5 (a)), it can be observed that the proliferation rates between two experimental groups have no significant difference during the period of measurements, and both are slower than the control group. However, as for the ones encapsulated in 4% alginate solution and its hydrogels, the proliferation behavior is very different. Although the experimental groups have lower cell survival rate compared to the ones in 2% alginate, the numbers of living cells significantly increased after 48 hours incubation with higher proliferation rate compared to the ones in 2% alginate. Furthermore, the proliferation rate of cells in high calcium concentration hydrogels is higher than the ones in low concentration group and control group. This surprising result might due to the exchange of calcium ions, which is an important second messenger signal in cell metabolism, between cells and their extracellular environments or the pH of the medium.

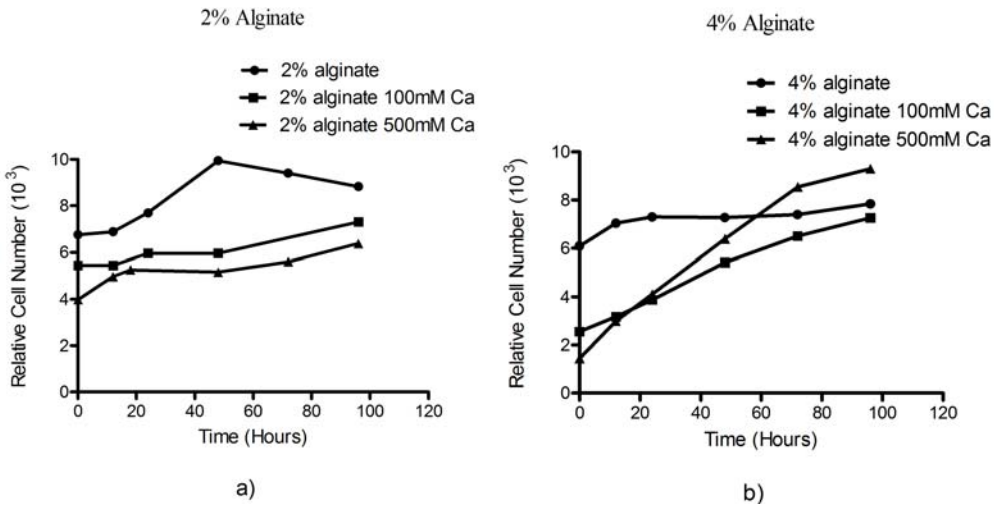


*Figure 4-5 Proliferation of encapsulated cells; a) cells in 2% alginate with calcium treatments, and b) cells in 4% alginate with calcium treatments, n=8*

### 4.3.3 Influence of Cell Density on Viscosity

Because the viscosity of the biopolymer solution influences both the scaffold fabrication process and cell damage, the viscosity of alginate solutions with varying cell densities was examined. As seen in Figure 4-6, the effect of cell density on solution viscosity was significant. Solution viscosity increased with both alginate concentration and cell density, and decreased with shear rate. Also, it is seen from Figure 4-6 that the cells density has different influences on the viscosity of the solution, depending on the alginate concentration. Specifically, the influence of cell density on viscosity in 4% alginate solution is more significant than that it is in 2% alginate solution.

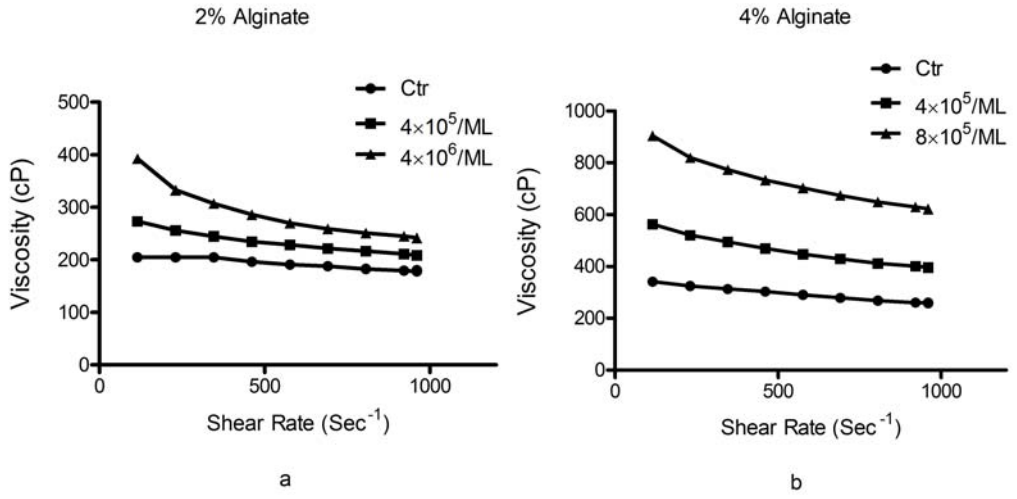


*Figure 4-6 Effect of cells density on viscosity of cell-alginate mixture with (a) 2% alginate and (b) 4% alginate, n=5, P<0.05*

## 4.4 Discussions

When cell damage happens, cells can either recover from the damage by its self-repair mechanism or continue to be dysfunctional even to the point of death, Depending on the degree of damage. In this process, the number of living cells would be balanced in a dynamic between cell death and proliferation. As for Schwann cell lines, the number of living cells should be doubled every 24 hours in a healthy normal proliferation rate. Thus, the number of living cells obtained from the experiments could indicate the degree of cell damage and their proliferation rate.

According to Figure 4-1 and Figure 4-2, all the cells in different group lost half of living cells when treated with calcium solutions. However, the degrees of damage on the remaining cells are different. Thus, the number of living cells treated with 100 mM calcium solution significantly increased 80% after 24 hours because of the recovery of damaged cells, while the ones in 1 M group continued to decrease to its 50%, in which most cells were dying within that time period. Although the proliferation rates of the cells treated with the lower calcium concentration were lower than those in the DMEM control group, the increasing number of living cells showed that the surviving cells were functionally active. The result also showed that the exposure time has a negative influence on the cell survival, which suggests the time period of using calcium chloride solution for crosslinking in the fabrication process must be limited.

Calcium ions are considered to be important in eukaryotic cell culture because they are involved with a wide range of vital cell functions including enzyme activities, attachment [151, 152], motility, tissue morphology, metabolic processes [153, 154], signal transduction [155, 156], replication, and electrochemical responses by specialized cells such as muscle and neural cells. By using Calcium ion as intracellular messenger, cells walk on a tightrope between life and death. A low calcium concentration (2 mM) must be maintained in the cytoplasm, and for most cells, calcium is stored in the endoplasmic reticulum (ER). A high calcium concentration is believed to damage the cell membrane by disturbing the state of cell electrolyte. However, because that it is noted in Figure 4-1 that the losses of living cells in groups treated with 1 M calcium were not different from those treated with 100 mM, which is the concentration should balance the osmosis stress. This result indicated that cell death happened in this process might be different than necrosis caused by osmosis stress. It is suggested that calcium ions had been used as obligatory signal for programmed cell death (or apoptosis) [157]. This hypothesis can be supported by the continuing cell death observed in Figure 4-2.

In Figure 4-3, the result showed that the number of cells are higher in 2% alginate solution than those in 4% alginate solution. This is possibly due to the reversible inhibition effect of 4% alginate solution on cells as previously reported, which might because of either its physical thickness or the hydrophilic properties of alginate [87]. As observed in the experiment, encapsulated cells rounded up instead of spreading out as they would when cultured in media, this prevented the formation of cell network and also the interactions between cells. At the same

time, cells might lack of interaction with alginate gel because its hydrophilic properties and lack of certain receptions for the proteins on the surface of cell membranes. Nevertheless, the results obtained suggests that low (i.e., 2%) concentration alginate solution is more suitable for cell encapsulation in engineering tissue scaffolds, as compared to high (i.e., 4%) concentration alginate solution.

In Figure 4-4, the proliferations of cells in both DMEM and alginate solution were influenced by cell density. The proliferation rate increased with the cell density, suggesting that cell density has a positive influence on cell proliferation. This might due to increased cell-cell chemical and biological stimulation for increasing the proliferation rate. When the cells were cultured at the same density, the proliferation rate of the cells in alginate solution was slower compared to those in DMEM; while the proliferation rate in 4% alginate was slower than the one in 2% alginate. This showed that the concentration of alginate had a negative influence on cell proliferation. The reason might be that the alginate slows down the absorption and exchanging of ions and proteins in the extracellular environment (as suggested in Figure 4-4 (d)), the encapsulated cells were more rounded in alginate and perhaps could not form regular cell-cell interactions as they did in DMEM alone. With increased cell density, the contact between cells increased thus the proliferation rate was higher.

In Figure 4-5, the proliferation of cells in alginate gel-suspension was observed. The ones encapsulated in 4% alginate solution and its hydrogels, the proliferation behavior is very different. Although the experimental groups have lower cell survival rate compared to the ones in 2% alginate, the numbers of living cells significantly increased after 48 hours incubation with higher proliferation rate compared to the ones in 2% alginate. Furthermore, the proliferation rate of cells in high calcium concentration hydrogels is higher than the ones in low concentration group and control group. This surprising result might due to the exchange of calcium ions, which play an important role in signaling in cell metabolism as second messenger and replication in cell reproduction, between cells and their extracellular environments. It has been reported that calcium can stimulate cell metabolism through certain receptors and pathways in mitochondrial $Ca^{2+}$ homeostasis [153]. Also, those released calcium ions might play important roles in DNA replication in mitosis process, which led to the increased number of cells in both 2% and 4% alginate hydrogels. Another hypothesis to explain this phenomenon is that those released calcium

ions might maintained the value of pH in the media, which trended to be turned into acidic solution by the chemicals produced and released by living cells in their metabolism process. This hypothesis can be affirmed by the changing of color in medium.

Figure 4-6 showed that solution viscosity increased with cell density. The results also illustrate the relationship between the cell density and the solution viscosity can be affected by the concentration of alginate solution, i.e., the higher the concentration, the more profound effect the cell density has on the solution viscosity. The reason for this might be because of the contact between cells caused by the contacts between proteins and receptions on the surface of cell membrane. The results present a dilemma situation in the scaffold fabrication, a higher cell density is required for the survival and proliferation in calcium abundant after fabrication, which, meanwhile, increases the solution viscosity and the mechanical forces needed in the scaffold fabrication, thus causing more cell damage. As such, further studies are encouraged to determine the cell density mixed in the solution such that desired cell survival proliferation rate can be achieved during the scaffold fabrication process and afterwards.

### 4.4 Conclusions

Cell survival and proliferation in alginate solution and its hydrogels were studied in this chapter in order to understand cell behavior within the calcium environment. The results show that the calcium concentration has a negative influence on cell survival rate. The number of surviving cells also decreased with the time exposed to calcium; longer exposure time leads to more cell damage. Furthermore, cells encapsulated in alginate hydrogels showed an interesting proliferation pattern. The proliferation rates of surviving cells in 2% alginate hydrogels do not differ much, regardless of the variation of calcium concentration. In contrast, the number of living cells increased significantly with calcium concentration in 4% alginate hydrogels.

The effect of cell density on the proliferation of encapsulated cells was also observed and studied in this chapter. The results showed that cell density, in the examined range, has a positive effect on cell proliferation. Cells as a kind of particles can influence the flow behavior and viscosity of alginate solution. As shown in this study, viscosity increased with cell density. Since increasing of viscosity could lead to more cell damage in the fabrication process as reported [125], it is necessary to find an appropriate cell density range for future study.

# Chapter 5 Summary, Conclusions, and Recommendations

## 5.1 Summary of the Research

A dispensing-based polymer deposition system was used to fabricate 3D porous hydrogel scaffolds. Sodium alginate had been chosen and used as a scaffolding biomaterial because of its good biocompatibility, and ease and fast gelation with divalent cations such as calcium ions. Calcium chloride was employed in this study as a crosslinker in order to form hydrogels with alginate solution. The mechanical properties of formed hydrogels were characterized and studied using compressive test in chapter 2. The results showed that the mechanical properties of the hydrogel could be controlled by the concentrations of alginate and calcium chloride. It was also demonstrated that the gelation time has a significantly impact on the mechanical properties of alginate hydrogel. Further, the study in this chapter investigated a post-fabrication treatment to strengthen formed hydrogels.

In chapter 3, the influence of fabrication process parameters such as pneumatic pressure, nozzle size, alginate concentration, and dispenser speeds on scaffold fabrication was studied. The optimal movement speed of the dispenser was determined experimentally with given pneumatic pressure, nozzle size, and alginate concentration in order to obtain diameters of the hydrogel struts that were close to the diameters of the nozzles used. With the knowledge and information gained from this study, 3D hydrogel scaffolds were successfully fabricated.

In chapter 4, the present study focused on the influence of calcium ions used as a crosslinker on cell viability and proliferation during and after the dispensing fabrication process. The influence of the concentration of calcium solutions and exposure time was studied on cells in both liquid medium and alginate hydrogel. Cell proliferation was studied for 96 hours in alginate hydrogels; the study showed that the density of alginate suspended cells and the alginate solution had a significant influence on cell proliferation. The study also showed that the density of encapsulated cells could affect the viscosity of alginate solution.

## 5.2 Discussion and Conclusions

The results of examining the mechanical properties of formed alginate hydrogels showed that the mechanical properties of alginate hydrogels increased with the reagent concentrations, and were also influenced by gelation time. The results obtained also showed that the mechanical properties of alginate hydrogels formed with low reagent concentration can be strengthened by a post-fabrication process, by which the hydrogel specimens were immersed in low concentration calcium chloride solution for a certain time period. The hydrogels formed through post-fabrication treatment were more elastic and had longer degradation time than the ones formed just by mixing the two reagents. The reason for this is that with longer gelation time, the guluronic residues in alginate polymer chain could form the maximal crosslink bonds with calcium ions, which strengthens the structure of the hydrogel. At the same time, with longer gelatin time in an aqueous environment, the hydrogel absorbed more water in the crosslink network, which also strengthened the hydrogel and gave more viscoelastic properties to the gel formed. The hydrogels formed with post-fabrication treatment showed some similarity with real tissues especially nerves (spinal cord or peripheral nerves) on their elastic modulus, and the mechanical properties of the hydrogels can be controlled and modified by controlling the reagents concentrations and gelation time.

The study also showed that the calcium chloride used as crosslinkers could cause cell damage even death, varying with the calcium concentration. The result presented in Chapter 4 showed that the cells could be exposed to calcium solution with a concentration of 500 mM for 30 min without permanent damaged and that the ones exposed to [1M] calcium solutions could be permanently damaged and lost their normal functions within 15 min. These results showed potentials but also limits for cell encapsulated tissue scaffold fabrication through dispensing method. An alternative way suggested by this study for overcoming the limits is to use the post-fabrication treatment discussed in Chapter 2. The scaffold can be fabricated by dispensing the alginate solution into the low concentration calcium chloride solution, and then the mechanical properties of the scaffold can be strengthened and modified through a post-fabrication treatment without the risk of permanently damaging the encapsulated cells. Furthermore, the results showed that the cell damage rate of encapsulated cells in 4% (w/v) alginate were greater than those encapsulated in 2% (w/v) alginate under the same condition, which suggested that the

mechanical forces within the alginate hydrogel network can damage the cells as well, compared to the results of mechanical properties study in chapter 2. The survival rate in 2% (w/v) alginate was close to those in DMEM, which indicated that the concentration of alginate solution for further study would be 2% (w/v).

The proliferation rate of encapsulated Schwann cells was measured and investigated in this study as well. The result in Chapter 4 also showed that the proliferation rate of Schwann cells was depending on both its density and alginate concentration if encapsulated in alginate solution. The proliferation rate increased with cell density and decreased with alginate concentration. However, if encapsulated in hydrogel, the proliferation rate differed from the one in alginate. The result showed that the number of cells in hydrogels formed with 4% (w/v) alginate increased significantly compared to the ones in 2% (w/v) alginate hydrogels. The reason for this result might due to the calcium ions released from the crosslink network of the hydrogel stimulating the growth or the crosslink the mechanical forces and isolation effects within the hydrogel less than the ones formed with 2% (w/v) alginate. More studies are needed to investigate the reason for this result. The influence of cell density on viscosity of alginate solution was also studied in Chapter 4. The results showed that the effects of cell density on alginate solution depended on the concentration of alginate solution, the higher the concentration was, the more significant of the effect would be. The result showed a dilemma of the scaffold fabrication, a higher cell density is required for the survival and proliferation in calcium abundant after fabrication, which, at the same time, would cause more shear stress and lead to more cell damage. Thus, further studies are needed to determine a range of cell density, within which the cell can have a reasonable survival rate during the dispensing fabrication process and a desirable proliferation rate after. It is noted that only Schwann cell line was employed in the present study. It is encouraged to pursue similar studies on other types of cells in order to have a more comprehensive understanding on cells responses to alginate hydrogel.

Also, the dispensing process of alginate solution was studied in Chapter 3. The concentration of alginate solution employed in this study was 2%, 3%, and 4% (w/v), and calcium chloride solution was used as crosslinker. The alginate solution was filled in a syringe and then extruded out by the pressurized air. The alginate was crosslinked by the calcium chloride reservoir as the dispenser moving along. The diameters of dispensed hydrogel struts depended on the

concentration of alginate solution, the height of the needle, and the diameter of the nozzle, the applied air pressure, and the speed of dispenser. More specifically, the diameter of the hydrogel strut increased with the diameter of the nozzle and the applied air pressure, and decreased with the concentration of alginate solution. Also, the diameter of the hydrogel struts depended on the horizontal moving speed If the speed were too slow, then the formed hydrogel strut would be curved, and in contrast, if the speed were too fast, then the formed hydrogel would be thin and even broken. Thus, the speed must be properly selected to achieve desired hydrogel strut. Combinations of these dispensing factors were used and studied for dispensing. Further than that, 3D hydrogel scaffolds were fabricated through dispensing method with 2% (w/v) alginate solution and 100 mM calcium chloride solution. The scaffolds were fabricated by the layer-by-layer method, in which each layer rotated 90° and was then formed on top of the other layers.

### 5.3 Future Work and Recommendations

In this study, the mechanical properties of hydrogels were characterized and measured by compressive test and compressive elastic modulus. The influence of mechanical properties on cell proliferation was discussed. However, the swollen and degradation properties were not examined in this thesis. These properties could influence the mechanical strength and the structural integrity, and furthermore how they change with the time. These remains to be studied in the future. This thesis also studied the survival of encapsulated cells and their proliferation. The number of cells in 4% (w/v) alginate hydrogel increased significantly compared to those in 2% alginate hydrogel. The reasons for this result need to be studied. Also, all the studies in this thesis were carried out *in vitro*. The mechanical properties, and the proliferation of cells should be further studied *in vivo*, so that the results would be more close to clinic conditions.

Also, the thesis showed that cell density would influence the viscosity of alginate solution significantly. Because the viscosity of alginate solution influence both scaffold structure formed and force-induced cell damage, thus a range of cell density need to be determined in the future study, within which the cell can have a reasonable survival rate during the dispensing fabrication process and a desirable proliferation rate after. The influence of the viscosity change caused by increasing cell density on the scaffold structure needs to be studied as well.

Furthermore, cell encapsulated tissue scaffold could be fabricated by dispensing technique based on the knowledge obtained from this thesis. The techniques for fabricating living cell

encapsulated tissue scaffolds and its applications to nerve tissue engineering need to be studied and discussed.

## LIST OF REFERENCES


1. Drury, J., *Hydrogels for tissue engineering: scaffold design variables and applications.* Biomaterials, 2003. 24(24): p. 4337-4351.
2. Stock, U.A. and J.P. Vacanti, *Tissue engineering: Current state and prospects.* Annual Review of Medicine, 2001. 52: p. 443-451.
3. Fuchs, J.R., B.A. Nasseri, and J.P. Vacanti, *Tissue engineering: A 21st century solution to surgical reconstruction.* Annals of Thoracic Surgery, 2001. 72(2): p. 577-591.
4. Wolfe, R.A., E.C. Roys, and R.M. Merion, *Trends in Organ Donation and Transplantation in the United States, 1999-2008.* American Journal of Transplantation, 2010. 10(4p2): p. 961-972.
5. SRTR, *Annual Report 2008.* http://ustransplan.org, 2010.
6. Yang, S., et al., *The design of scaffolds for use in tissue engineering. Part 1. Traditional factors.* Tissue Engineering, 2001: p. 679-689.
7. Lee, K.Y. and D.J. Mooney, *Hydrogels for Tissue Engineering.* Chemical Reviwes, 2001. 101(7).
8. Ramay, H.R.R. and M. Zhang, *Biphasic calcium phosphate nanocomposite porous scaffolds for load-bearing bone tissue engineering.* Biomaterials, 2004. 25(21): p. 5171-5180.
9. Salvay, D.M., M. Zelivyanskaya, and L.D. Shea, *Gene delivery by surface immobilization of plasmid to tissue-engineering scaffolds.* Gene Therapy, 2010. 17(9): p. 1134-1141.
10. Yin, G.B., et al., *Study on the Electrospun PLA/silk Fibroin-Gelatin Composite Nanofibrous Scaffold for Tissue Engineering.* 2008 International Symposium on Fiber Based Scaffolds for Tissue Engineering, Proceedings, 2008: p. 284-289

303.

11. Duarte, A.R.C., J.F. Mano, and R.L. Reis, *Novel 3D scaffolds of chitosan-PLLA blends for tissue engineering applications: Preparation and characterization.* Journal of Supercritical Fluids, 2010. 54(3): p. 282-289.
12. Dey, J., et al., *Crosslinked urethane doped polyester biphasic scaffolds: Potential for in vivo vascular tissue engineering.* Journal of Biomedical Materials Research Part A, 2010. 95A(2): p. 361-370.

13. Nojehdehian, H., et al., *Effect of poly-L-lysine coating on retinoic acid-loaded PLGA microspheres in the differentiation of carcinoma stem cells into neural cells.* International Journal of Artificial Organs, 2010. 33(10): p. 721-730.
14. Weikel, A.L., et al., *Miscibility of choline-substituted polyphosphazenes with PLGA and osteoblast activity on resulting blends.* Biomaterials, 2010. 31(33): p. 8507-8515.
15. Zhou, X.G., et al., *In vitro hydrolytic and enzymatic degradation of nestlike-patterned electrospun poly(D,L-lactide-co-glycolide) scaffolds.* Journal of Biomedical Materials Research Part A, 2010. 95A(3): p. 755-765.
16. Alvarez-Barreto, J.F., et al., *Enhanced osteoblastic differentiation of mesenchymal stem cells seeded in RGD-functionalized PLLA scaffolds and cultured in a flow perfusion bioreactor.* J Tissue Eng Regen Med.
17. Hurtado, A., et al., *Poly (d,l-lactic acid) macroporous guidance scaffolds seeded with Schwann cells genetically modified to secrete a bi-functional neurotrophin implanted in the completely transected adult rat thoracic spinal cord.* Biomaterials, 2006. 27(3): p. 430-442.
18. Li, Z., et al., *Chitosan/alginate hybrid scaffolds for bone tissue engineering.* Biomaterials, 2005. 26(18): p. 3919-3928.
19. Shachaf, Y., M. Gonen-Wadmany, and D. Seliktar, *The biocompatibility of PluronicF127 fibrinogen-based hydrogels.* Biomaterials. 31(10): p. 2836-47.
20. Mohan, N. and P.D. Nair, *A synthetic scaffold favoring chondrogenic phenotype over a natural scaffold.* Tissue Eng Part A. 16(2): p. 373-84.
21. Khatayevich, D., et al., *Biofunctionalization of materials for implants using engineered peptides.* Acta Biomaterialia. 6(12): p. 4634-4641.
22. Stokols, S. and M.H. Tuszynski, *Freeze-dried agarose scaffolds with uniaxial channels stimulate and guide linear axonal growth following spinal cord injury.* Biomaterials, 2006. 27(3): p. 443-451.
23. Kozulic, B., *Looking at bands from another side.* Anal Biochem, 1994. 216(2): p. 253-61.
24. Afshin Mosahebi, M.S., Mikael Wiberg, Giorgio Terenghi, *A Novel Use of Alginate Hydrogel as Schwann Cell Matrix.* Tissue Eng, 2001. 7(5).
25. Kataoka, K., et al., *Alginate enhances elongation of early regenerating axons in spinal cord of young rats.* Tissue Engineering, 2004. 10(3-4): p. 493-504.

26. Cardea, S., P. Pisanti, and E. Reverchon, *Generation of chitosan nanoporous structures for tissue engineering applications using a supercritical fluid assisted process.* Journal of Supercritical Fluids, 2010. 54(3): p. 290-295.
27. Kang, Y.M., et al., *In Vivo Biocompatibility Study of Electrospun Chitosan Microfiber for Tissue Engineering.* International Journal of Molecular Sciences, 2010. 11(10): p. 4140-4148.
28. Goto, E., et al., *A rolled sheet of collagen gel with cultured Schwann cells: Model of nerve conduit to enhance neurite growth.* Journal of Bioscience and Bioengineering, 2010. 109(5): p. 512-518.
29. Chen, G.P., T. Ushida, and T. Tateishi, *A biodegradable hybrid sponge nested with collagen microsponges.* Journal of Biomedical Materials Research, 2000. 51(2): p. 273-279.
30. Xiaohong, W., et al., *Design and Fabrication of PLGA Sandwiched Cell/Fibrin Constructs for Complex Organ Regeneration.* Journal of Bioactive and Compatible Polymers, 2010. 25(3): p. 229-240.
31. Bryant, S. and K. Anseth, *The effects of scaffold thickness on tissue engineered cartilage in photocrosslinked poly(ethylene oxide) hydrogels.* Biomaterials, 2001: p. 619-626.
32. Ogata, N., *Advanced biomaterials in biomedical engineering and drug delivery systems*. 1996, Tokyo ; New York: Springer. xxiv, 381 p.
33. Liu, Y., et al., *Hyaluronic acid-gelatin fibrous scaffold produced by electrospinning of their aqueous solution for tissue engineering applications.* Advances in Material Design for Regenerative Medicine, Drug Delivery and Targeting/Imaging, 2009. 1140: p. 131-136

223.

34. Bencherif, S.A., et al., *Bioresorbable hyaluronic acid hydrogels for tissue engineering applications.* Abstracts of Papers of the American Chemical Society, 2008. 236: p. -.
35. L.W.Chan, Y.J., P.W.S. Heng, *Cross-linking mechanisms of calcium and zinc in production of alginate microspheres.* International Journal of Pharmaceutics, 2002. 242.
36. Bryant, S.J. and K.S. Anseth, *The e!ects of sca!old thickness on tissue engineered cartilage in photocrosslinked poly(ethylene oxide) hydrogels.* Biomaterials, 2001. 22.

37. Prestwich, G.D., *Evaluating drug efficacy and toxicology in three dimensions: using synthetic extracellular matrices in drug discovery.* Acc Chem Res, 2008. 41(1): p. 139-48.
38. Munjeri, O., et al., *An investigation into the suitability of amidated pectin hydrogel beads as a delivery matrix for chloroquine.* J Pharm Sci, 1998. 87(8): p. 905-8.
39. Cartmell, S., *Controlled Release Scaffolds for Bone Tissue Engineering.* Journal of Pharmaceutical Sciences, 2009. 98(2): p. 430-441.
40. Eckert, C.E., et al., *Three-Dimensional Quantitative Micromorphology of Pre- and Post-Implanted Engineered Heart Valve Tissues.* Ann Biomed Eng.
41. Cai, Y.Z., et al., *Electrospun nanofibrous matrix improves the regeneration of dense cortical bone.* J Biomed Mater Res A. 95(1): p. 49-57.
42. Lin, Q., et al., *Anti-washout carboxymethyl chitosan modified tricalcium silicate bone cement: preparation, mechanical properties and in vitro bioactivity.* J Mater Sci Mater Med. 21(12): p. 3065-76.
43. Miranda, S.C., et al., *Three-dimensional culture of rat BMMSCs in a porous chitosan-gelatin scaffold: A promising association for bone tissue engineering in oral reconstruction.* Arch Oral Biol.
44. Wang, W.H., et al., *Cross-linked Collagen-Chondroitin Sulfate-Hyaluronic Acid Imitating Extracellular Matrix as Scaffold for Dermal Tissue Engineering.* Tissue Engineering Part C-Methods, 2010. 16(2): p. 269-279.
45. Kobus, K.F. and T. Dydymski, *Quantitative dermal measurements following treatment with AirGent.* Aesthet Surg J. 30(5): p. 725-9.
46. Yu, J., et al., *The use of human mesenchymal stem cells encapsulated in RGD modified alginate microspheres in the repair of myocardial infarction in the rat.* Biomaterials, 2010. 31(27): p. 7012-7020.
47. Gavini, E., et al., *Mucoadhesive vaginal tablets as veterinary delivery system for the controlled release of an antimicrobial drug, acriflavine.* AAPS PharmSciTech, 2002. 3(3): p. E20.
48. Andrade, L.R., et al., *Fine structure and molecular content of human chondrocytes encapsulated in alginate beads.* Cell Biol Int.

49. Cohen, D.L., et al., *Additive manufacturing for in situ repair of osteochondral defects.* Biofabrication, 2010. 2(3): p. 035004.
50. Miranda, J.P., et al., *Extending hepatocyte functionality for drug-testing applications using high-viscosity alginate-encapsulated three-dimensional cultures in bioreactors.* Tissue Eng Part C Methods. 16(6): p. 1223-32.
51. Lan, S.-F., B. Safiejko-Mroczka, and B. Starly, *Long-term cultivation of HepG2 liver cells encapsulated in alginate hydrogels: A study of cell viability, morphology and drug metabolism.* Toxicology in Vitro, 2010. 24(4): p. 1314-1323.
52. McGrath, A.M., et al., *BD PuraMatrix peptide hydrogel seeded with Schwann cells for peripheral nerve regeneration.* Brain Res Bull. 83(5): p. 207-13.
53. Allan, C.H., *Functional results of primary nerve repair.* Hand Clinics, 2000. 16(1): p. 67-+.
54. Vanderhooft, E., *Functional outcomes of nerve grafts for the upper and lower extremities.* Hand Clinics, 2000. 16(1): p. 93-+.
55. Cai, S., et al., *Derivation of Clinically Applicable Schwann Cells from Bone Marrow Stromal Cells for Neural Repair and Regeneration.* Cns & Neurological Disorders-Drug Targets, 2011. 10(4): p. 500-508.
56. Li, X., et al., *Repair of thoracic spinal cord injury by chitosan tube implantation in adult rats.* Biomaterials, 2009. 30(6): p. 1121-1132.
57. King-Robson, J., *Encouraging regeneration in the central nervous system: Is there a role for olfactory ensheathing cells?* Neuroscience Research, 2011. 69(4): p. 263-275.
58. Gueye, Y., et al., *Trafficking and Secretion of Matrix Metalloproteinase-2 in Olfactory Ensheathing Glial Cells: A Role in Cell Migration?* Glia, 2011. 59(5): p. 750-770.
59. Munro, K.M. and V.M. Perreau, *Current and Future Applications of Transcriptomics for Discovery in CNS Disease and Injury.* Neurosignals, 2009. 17(4): p. 311-327.
60. Tabesh, H., et al., *The role of biodegradable engineered scaffolds seeded with Schwann cells for spinal cord regeneration.* Neurochemistry International, 2009. 54(2): p. 73-83.
61. Deng, L.X., et al., *GDNF modifies reactive astrogliosis allowing robust axonal regeneration through Schwann cell-seeded guidance channels after spinal cord injury.* Experimental Neurology, 2011. 229(2): p. 238-250.

62. Draget, K.I., et al., *Swelling and partial solubilization of alginic acid gel beads in acidic buffer.* Carbohydrate Polymers, 1996. 29(3): p. 209-215.
63. Petra Eiselt, K.Y.L., and David J. Mooney, *Rigidity of Two-Component Hydrogels Prepared from Alginate and Poly(ethylene glycol)-Diamines.* Macromolecules, 1999. 32.
64. Kim, J.O., et al., *Development of Clindamycin-Loaded Wound Dressing with Polyvinyl Alcohol and Sodium Alginate.* Biological & Pharmaceutical Bulletin, 2008. 31(12): p. 2277-2282.
65. Pielesz, A., B. Katarzyna, and M. Klimczak, *Physico-chemical properties of commercial active alginate dressings.* Polim Med, 2008. 38(4): p. 3-17.
66. Ubbink, D.T., et al., *Topical negative pressure for treating chronic wounds.* Cochrane Database of Systematic Reviews, 2008(3): p. -.
67. Tarawneh, F.M., P.G. Panos, and A.E. Athanasiou, *Three-dimensional assessment of dental casts' occlusal surfaces using two impression materials.* Journal of Oral Rehabilitation, 2008. 35(11): p. 821-826.
68. Ohtani, M., et al., *Indication and limitations of using palatal rugae for personal identification in edentulous cases.* Forensic Science International, 2008. 176(2-3): p. 178-182.
69. de Guzman, R.C., et al., *Alginate-matrigel microencapsulated schwann cells for inducible secretion of glial cell line derived neurotrophic factor.* J Microencapsul, 2008. 25(7): p. 487-98.
70. Lewis, A.S. and Massachusetts Institute of Technology. Dept. of Chemical Engineering., *Eliminating oxygen supply limitations for transplanted microencapsulated islets in the treatment of type 1 diabetes*. 2008. p. 234 p.
71. Liang, Y., et al., *An in situ formed biodegradable hydrogel for reconstruction of the corneal endothelium.* Colloids and Surfaces B-Biointerfaces, 2011. 82(1): p. 1-7.
72. Kikuchi, A. and T. Okano, *Pulsatile drug release control using hydrogels.* Advanced Drug Delivery Reviews, 2002. 54(1): p. 53-77.
73. Pandey, R. and K. G, - *Alginate as a Drug Delivery Carrier.* 2005. - null.
74. Jon A. Rowley!, G.M., David J. Mooney, *Alginate hydrogels as synthetic extracellular matrix materials.* Biomaterials, 1999. 20.

75. Russell, B.B., *The degradation of sodium alginate on drying / by Barrett B. Russell, 3rd*. 1943. p. 22, [26] leaves.
76. Lee, K.Y., K.H. Bouhadir, and D.J. Mooney, *Degradation behavior of covalently cross-linked poly(aldehyde guluronate) hydrogels.* Macromolecules, 2000. 33(1): p. 97-101.
77. Kamal H. Bouhadir, K.Y.L., Eben Alsberg, Kelly L. Damm, Kenneth W. Anderson, and David J. Mooney, *Degradation of Partially Oxidized Alginate and Its Potential Application for Tissue Engineering.* Biotechnol Prog, 2001. 17.
78. Lee, J.W., et al., *The effect of spacer arm length of an adhesion ligand coupled to an alginate gel on the control of fibroblast phenotype.* Biomaterials, 2010. 31(21): p. 5545-5551.
79. Wu, M.Y., et al., *Chitosan/Alginate Multilayer Scaffold Encapsulating Bone Marrow Stromal Cells In Situ on Titanium.* Journal of Bioactive and Compatible Polymers, 2009. 24(4): p. 301-315.
80. Liu, X., et al., *Swelling behaviour of alginate–chitosan microcapsules prepared by external gelation or internal gelation technology.* Carbohydrate Polymers, 2004. 56(4): p. 459-464.
81. Hui Ling Lai, A.A.K., Duncan Q.M. Craig, *The preparation and characterisation of drug-loaded alginate and chitosan sponges.* International Journal of Pharmaceutics, 2003. 251.
82. Zhang, Y., et al., *Preparation and evaluation of alginate-chitosan microspheres for oral delivery of insulin.* Eur J Pharm Biopharm, 2010.
83. Landa, N., et al., *Effect of injectable alginate implant on cardiac remodeling and function after recent and old infarcts in rat.* Circulation, 2008. 117(11): p. 1388-96.
84. Leor, J., et al., *Intracoronary injection of in situ forming alginate hydrogel reverses left ventricular remodeling after myocardial infarction in Swine.* J Am Coll Cardiol, 2009. 54(11): p. 1014-23.
85. Cohen, D.L., et al., *Direct freeform fabrication of seeded hydrogels in arbitrary geometries.* Tissue Eng, 2006. 12(5): p. 1325-35.
86. Banerjee, A., et al., *The influence of hydrogel modulus on the proliferation and differentiation of encapsulated neural stem cells.* Biomaterials, 2009. 30(27): p. 4695-4699.

87. Hunt, N.C., R.M. Shelton, and L.M. Grover, *Reversible mitotic and metabolic inhibition following the encapsulation of fibroblasts in alginate hydrogels.* Biomaterials, 2009. 30(32): p. 6435-6443.
88. Dhollander, A.A.M., et al., *MRI evaluation of a new scaffold-based allogenic chondrocyte implantation for cartilage repair.* European Journal of Radiology, 2010. 75(1): p. 72-81.
89. Lee, K.Y., K.H. Bouhadir, and D.J. Mooney, *Controlled degradation of hydrogels using multi-functional cross-linking molecules.* Biomaterials, 2004. 25(13): p. 2461-2466.
90. Davidovich-Pinhas, M. and H. Bianco-Peled, *Alginate-PEGAc: A new mucoadhesive polymer.* Acta Biomater.
91. Hall, K.K., K.M. Gattas-Asfura, and C.L. Stabler, *Microencapsulation of islets within alginate/poly(ethylene glycol) gels cross-linked via Staudinger ligation.* Acta Biomater.
92. Kuen Yong Lee, J.A.R., Petra Eiselt, Erick M. Moy, Kamal H. Bouhadir, and David J. Mooney, *Controlling Mechanical and Swelling Properties of Alginate Hydrogels Independently by Cross-Linker Type and Cross-Linking Density.* Macromolecules, 2000. 33.
93. Donati, I., et al., *New hypothesis on the role of alternating sequences in calcium-alginate gels.* Biomacromolecules, 2005. 6(2): p. 1031-1040.
94. University, L.S.B., *Water Structure and Science.* http://www.lsbu.ac.uk/water/index2.html.
95. Drury, J., *The tensile properties of alginate hydrogels.* Biomaterials, 2004. 25(16): p. 3187-3199.
96. LeRoux, M.A., F. Guilak, and L.A. Setton, *Compressive and shear properties of alginate gel: effects of sodium ions and alginate concentration.* J Biomed Mater Res, 1999. 47(1): p. 46-53.
97. Awad, H.A., et al., *Chondrogenic differentiation of adipose-derived adult stem cells in agarose, alginate, and gelatin scaffolds.* Biomaterials, 2004. 25(16): p. 3211-22.
98. Laurencin, C.T. and L.S. Nair, *Nanotechnology and tissue engineering the scaffold*. 2008, CRC Press: Boca Raton.

99. Barillaro, V., et al., *High-throughput study of phenytoin solid dispersions: Formulation using an automated solvent casting method, dissolution testing, and scaling-up.* Journal of Combinatorial Chemistry, 2008. 10(5): p. 637-643.
100. Shanbhag, A., et al., *Method for screening of solid dispersion formulations of low-solubility compounds - Miniaturization and automation of solvent casting and dissolution testing.* International Journal of Pharmaceutics, 2008. 351(1-2): p. 209-218.
101. Lim, J.I., et al., *Preparation of Interconnected Porous Chitosan Scaffolds by Sodium Acetate Particulate Leaching.* J Biomater Sci Polym Ed.
102. Laschke, M.W., et al., *In vitro and in vivo evaluation of a novel nanosize hydroxyapatite particles/poly(ester-urethane) composite scaffold for bone tissue engineering.* Acta Biomater. 6(6): p. 2020-7.
103. Salerno, A., et al., *Design of porous polymeric scaffolds by gas foaming of heterogeneous blends.* J Mater Sci Mater Med, 2009. 20(10): p. 2043-51.
104. Zhu, X.H., et al., *Characterization of porous poly(D,L-Lactic-co-glycolic acid) sponges fabricated by supercritical CO2 gas-foaming method as a scaffold for three-dimensional growth of hep3B cells.* Biotechnology and Bioengineering, 2008. 100(5): p. 998-1009.
105. Salerno, A., S. Iannace, and P.A. Netti, *Open-pore biodegradable foams prepared via gas foaming and microparticulate templating.* Macromolecular Bioscience, 2008. 8(7): p. 655-664.
106. Huang, Y.L., et al., *One dimensional molecular dipole chain arrays on graphite via nanoscale phase separation.* Chem Commun (Camb). 46(47): p. 9040-2.
107. Vellaichamy, S. and K. Palanivelu, *Preconcentration and separation of copper, nickel and zinc in aqueous samples by flame atomic absorption spectrometry after column solid-phase extraction onto MWCNTs impregnated with D2EHPA-TOPO mixture.* J Hazard Mater.
108. Allo, B.A., A.S. Rizkalla, and K. Mequanint, *Synthesis and Electrospinning of epsilon-Polycaprolactone-Bioactive Glass Hybrid Biomaterials via a Sol-Gel Process.* Langmuir. 26(23): p. 18340-8.
109. Agarwal, S., J.H. Wendorff, and A. Greiner, *Progress in the field of electrospinning for tissue engineering applications.* Adv Mater, 2009. 21(32-33): p. 3343-51.

110. Park, S.M., et al., *Rapid Prototyping of Nanofluidic Systems Using Size-Reduced Electrospun Nanofibers for Biomolecular Analysis.* Small, 2010.

111. Liu, Y.F., X.T. Dong, and F.D. Zhu, *Overview of Rapid Prototyping for Fabrication of Bone Tissue Engineering Scaffold.* Digital Design and Manufacturing Technology, Pts 1 and 2, 2010. 102-104: p. 550-554

964.

112. Oh, S.H., et al., *Fabrication and characterization of hydrophilic poly(lactic-co-glycolic acid)/poly(vinyl alcohol) blend cell scaffolds by melt-molding particulate-leaching method.* Biomaterials, 2003. 24(22): p. 4011-4021.

113. Oh, S.H., S.G. Kang, and J.H. Lee, *Degradation behavior of hydrophilized PLGA scaffolds prepared by melt-molding particulate-leaching method: Comparison with control hydrophobic one.* Journal of Materials Science-Materials in Medicine, 2006. 17(2): p. 131-137.

114. Lewis, L.M., et al., *Characterizing the Freeze-Drying Behavior of Model Protein Formulations.* AAPS PharmSciTech.

115. Huang, Q., et al., *Preliminary separation of the growth factors in platelet-rich plasma: effects on the proliferation of human marrow-derived mesenchymal stem cells.* Chin Med J (Engl), 2009. 122(1): p. 83-7.

116. Aramwit, P., et al., *Formulation and characterization of silk sericin-PVA scaffold crosslinked with genipin.* Int J Biol Macromol. 47(5): p. 668-75.

117. Azami, M., F. Orang, and F. Moztarzadeh, *Nanocomposite bone tissue-engineering scaffolds prepared from gelatin and hydroxyapatite using layer solvent casting and freeze-drying technique.* 2006 International Conference on Biomedical and Pharmaceutical Engineering, Vols 1 and 2, 2006: p. 259-264

596.

118. Guess, P.C., et al., *Monolithic CAD/CAM Lithium Disilicate Versus Veneered Y-TZP Crowns: Comparison of Failure Modes and Reliability After Fatigue.* Int J Prosthodont, 2010. 23(5): p. 434-42.

119. Khallaghi, S., et al., *Registration of a statistical shape model of the lumbar spine to 3D ultrasound images.* Med Image Comput Comput Assist Interv, 2010. 13(Pt 2): p. 68-75.

120. Khalil, S. and W. Sun, *Bioprinting Endothelial Cells With Alginate for 3D Tissue Constructs.* Journal of Biomechanical Engineering, 2009. 131(11): p. 111002.
121. Chang, R. and W. Sun, *Effects of dispensing pressure and nozzle diameter on cell survival from solid freeform fabrication-based direct cell writing.* Tissue Engineering Part A, 2008. 14(1): p. 41-48.
122. Wang, X.H., et al., *Generation of three-dimensional hepatocyte/gelatin structures with rapid prototyping system.* Tissue Engineering, 2006. 12(1): p. 83-90.
123. Shengjie, L., et al., *Direct Fabrication of a Hybrid Cell/Hydrogel Construct by a Double-nozzle Assembling Technology.* Journal of Bioactive and Compatible Polymers, 2009. 24(3): p. 249-265.
124. Hu, M., et al., *Hydrodynamic spinning of hydrogel fibers.* Biomaterials, 2010. 31(5): p. 863-869.
125. Li, M.G., X.Y. Tian, and X.B. Chen, *A brief review of dispensing-based rapid prototyping techniques in tissue scaffold fabrication: role of modeling on scaffold properties prediction.* Biofabrication, 2009. 1(3).
126. Vozzi, G., et al., *Fabrication of PLGA scaffolds using soft lithography and microsyringe deposition.* Biomaterials, 2003. 24(14): p. 2533-2540.
127. Lam, C.X.F., et al., *Scaffold development using 3D printing with a starch-based polymer.* Materials Science & Engineering C-Biomimetic and Supramolecular Systems, 2002. 20(1-2): p. 49-56.
128. Xiong, Z., et al., *Fabrication of porous poly(L-lactic acid) scaffolds for bone tissue engineering via precise extrusion.* Scripta Materialia, 2001. 45(7): p. 773-779.
129. Chen, X.B., G. Schoenau, and W.J. Zhang, *On the flow rate dynamics in time-pressure dispensing processes.* Journal of Dynamic Systems Measurement and Control-Transactions of the Asme, 2002. 124(4): p. 693-698.
130. Khalil, S.E.D., *Deposition and Structural Formation of 3D Alginate Tissue Scaffolds*, in *Mechanical Engineering*. 2005, Derexl University.
131. Niavarani, A. and N.V. Priezjev, *Modeling the combined effect of surface roughness and shear rate on slip flow of simple fluids.* Physical Review E, 2010. 81(1): p. -.

132. Gupta, A.K. and A.S.G. Curtis, *Surface modified superparamagnetic nanoparticles for drug delivery: Interaction studies with human fibroblasts in culture.* Journal of Materials Science-Materials in Medicine, 2004. 15(4): p. 493-496.

133. Schmid, G., *Nanoparticles : from theory to application*. 2004, Weinheim Chichester: Wiley-VCH ; Wiley distributor. x, 434 p.

134. Al-Somali, A.M., et al., *Recycling size exclusion chromatography for the analysis and separation of nanocrystalline gold.* Anal Chem, 2004. 76(19): p. 5903-10.

135. Xu, M., et al., *An cell-assembly derived physiological 3D model of the metabolic syndrome, based on adipose-derived stromal cells and a gelatin/alginate/fibrinogen matrix.* Biomaterials, 2010. 31(14): p. 3868-3877.

136. Suarez-Gonzalez, D., et al., *Controlled nucleation of hydroxyapatite on alginate scaffolds for stem cell-based bone tissue engineering.* Journal of Biomedical Materials Research Part A, 2010. 95A(1): p. 222-234.

137. Spirnak, J.P., et al., *GADOLINIUM-ENHANCED MAGNETIC-RESONANCE-IMAGING ASSESSMENT OF HYDROXYAPATITE ORBITAL IMPLANTS.* American Journal of Ophthalmology, 1995. 119(4): p. 431-440.

138. Ino, K., A. Ito, and H. Honda, - *Cell patterning using magnetite nanoparticles and magnetic force.* 2007. - 97(- 5): p. - 1317.

139. Frasca, G., F. Gazeau, and C. Wilhelm, *Formation of a Three-Dimensional Multicellular Assembly Using Magnetic Patterning.* Langmuir, 2009. 25(4): p. 2348-2354.

140. Smith, C.M., et al., *Characterizing environmental factors that impact the viability of tissue-engineered constructs fabricated by a direct-write bioassembly tool.* Tissue Eng, 2007. 13(2): p. 373-83.

141. Li, M., et al., *Modeling process-induced cell damage in the biodispensing process.* Tissue Eng Part C Methods. 16(3): p. 533-42.

142. Wan, L.Q., et al., *Calcium Concentration Effects on the Mechanical and Biochemical Properties of Chondrocyte-Alginate Constructs.* Cell Mol Bioeng, 2008. 1(1): p. 93-102.

143. Bose, *ElectroForce® 3100 Test Instruments Brochure.* http://www.bose-electroforce.com/product.cfm?pid=41&sid=1.

144. Ozawa, H., et al., *Mechanical properties and function of the spinal pia mater.* Journal of Neurosurgery-Spine, 2004. 1(1): p. 122-127.

145. Edward L. Mazuchowski, L.E.T., *Biomechanical properties of the human spinal cord and pia mater*, in *2003 Summer Bioengineering Conference*. 2003: Sonesta Beach Resort in Key Biscayne, Fiorida.
146. Chen, X.B., M.G. Li, and H. Ke, *Modeling of the Flow Rate in the Dispensing-Based Process for Fabricating Tissue Scaffolds.* Journal of Manufacturing Science and Engineering, 2008. 130(2): p. 021003.
147. Khalil, S.E.D. and W. Sun, *Deposition and structural formation of 3D alginate tissue scaffolds*. 2005, Drexel University: Philadelphia, Pa. p. xxi, 251 leaves.
148. Yan, K.C., K. Nair, and W. Sun, *Three dimensional multi-scale modelling and analysis of cell damage in cell-encapsulated alginate constructs.* J Biomech. 43(6): p. 1031-8.
149. Mosmann, T., *Rapid colorimetric assay for cellular growth and survival: Application to proliferation and cytotoxicity assays.* Journal of Immunological Methods, 1983. - 65(- 1-2): p. - 63.
150. Inc, C., *Molecular Devices SPECTRAmax 250 Product Description.* http://www.gmi-inc.com/Molecular-Devices-SpectraMax-250-Microplate-Reader.html, 2007.
151. Lawler, J., R. Weinstein, and R.O. Hynes, *Cell Attachment to Thrombospondin - the Role of Arg-Gly-Asp, Calcium, and Integrin Receptors.* Journal of Cell Biology, 1988. 107(6): p. 2351-2361.
152. Abou Neel, E.A., et al., *Chemical, modulus and cell attachment studies of reactive calcium phosphate filler-containing fast photo-curing, surface-degrading, polymeric bone adhesives.* Acta Biomaterialia, 2010. 6(7): p. 2695-2703.
153. Rimessi, A., et al., *The versatility of mitochondrial calcium signals: From stimulation of cell metabolism to induction of cell death.* Biochimica Et Biophysica Acta-Bioenergetics, 2008. 1777(7-8): p. 808-816.
154. Murgia, M., et al., *Controlling metabolism and cell death: At the heart of mitochondrial calcium signalling.* Journal of Molecular and Cellular Cardiology, 2009. 46(6): p. 781-788.
155. Chattree, V., N. Khanna, and D.N. Rao, *Alterations in T cell signal transduction by M-leprae antigens is associated with downregulation of second messengers PKC, calcium, calcineurin, MAPK and various transcription factors in leprosy patients.* Molecular Immunology, 2007. 44(8): p. 2066-2077.

156. Xu, J., et al., *Evidence of reciprocal regulation between the high extracellular calcium and RANKL signal transduction pathways in RAW cell derived osteoclasts.* Journal of Bone and Mineral Research, 2004. 19: p. S419-S419.

157. Demaurex, N. and C. Distelhorst, *Apoptosis - the calcium connection.* Science, 2003. 300(5616): p. 65-67.